TECHNISCHE UNIVERSITÄT WIEN
Vienna University of Technology

DIPLOMARBEIT

Constrained rhombic nets — discrete differential geometry and applications

Ausgeführt am Institut für
Diskrete Mathematik und Geometrie
der Technischen Universität Wien

unter der Anleitung von Prof. Dr. Helmut Pottmann

durch

Florian Käferböck

Andreas Hofer Gasse 36/1, A-2340 Mödling

Datum

Unterschrift

Contents

Introduction

A parametrization of a two-dimensional differentiable surface $f : U \subseteq \mathbb{R}^2 \to \mathbb{R}^3$ is called a *Chebychev net* if for rectangles $[a_0, a_1] \times [b_0, b_1]$ the lengths of the curves $f([a_0, a_1], b_0)$ and $f([a_0, a_1], b_1)$, as well as $f(a_0, [b_0, b_1])$ and $f(a_1, [b_0, b_1])$ are equal. By doing a simple linear coordinate transform we can without loss of generality describe Chebychev nets as those nets with

$$\|f_{u_1}(u)\| = \|f_{u_2}(u)\| = 1 \ \forall u \in U.$$

From this we see that the discrete analoga of Chebychev nets are discrete rhombic nets, that is nets whose faces are all rhombi.

All differentiable surfaces can be at least locally described by Chebychev nets. The discrete analogy is that it is possible to (once again, possibly only locally) approximate a given surface with a discrete rhombic mesh.

The second section of this thesis is concerned with this problem. We will describe and analyze algorithms that lay a (finite) rhombic mesh on a given triangle mesh. It is emphasized that these algorithms are targeted for implementation on a computer system for practical use.

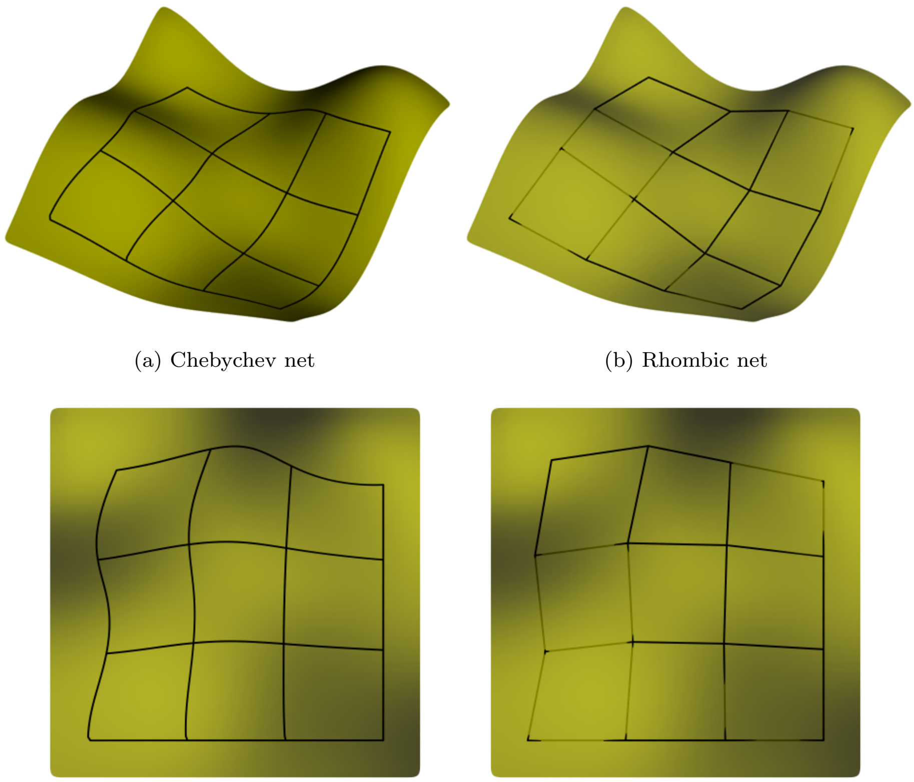

(a) Chebychev net

(b) Rhombic net

(c) Chebychev net

(d) Rhombic net

Figure 1: Surface overlayed with Chebychev and rhombic nets

(For example the Chebychev net in figure (1) was (approximatively) calculated by using the implementation of the algorithms in section (2) to construct a very fine rhombic mesh and print only every 20th row and column.)

Differentiable surfaces with constant negative Gaussian curvatures are called *pseudospheres*. In differental geometry it is shown that they are just the surfaces whose asymptotic curves form a Chebyshev net. Surfaces like that were studied extensively in the first half of the 20th century and even earlier. Around 1950 W. Wunderlich among others considered the topic from the point of view of discrete differential geometry. It was found that the discrete analoga of pseudospheric surfaces with Chebyshev parametrizations are rhombic meshes with planar knots, that is rhombic meshes where the four edges emanating from each knot lie in a common plane. They also result as stationary configurations if a rhombic mesh of ropes is strung out under certain configurations of forces on the border knots.

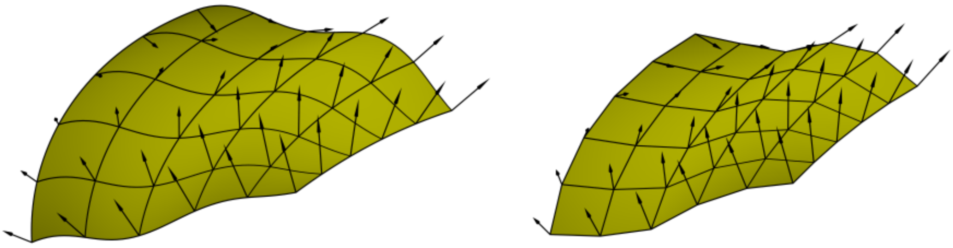

(a) Pseudospheric surface

(b) Rhombic net with planar knots

Figure 2: Pseudospheric surface and discrete analogon

The first section of this thesis will display some results of (W. Wunderlich 1952). They will also be extended to *rhombic meshes with conical knots of uniform aperture* (called shortly *rhombic-conical meshes*), which will be shown to be offset surfaces of rhombic meshes with planar knots.

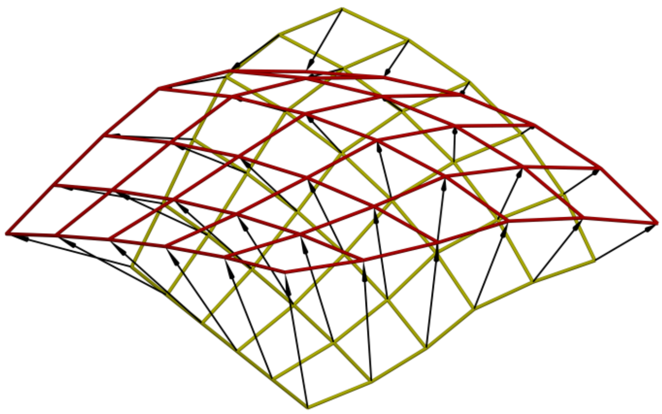

Figure 3: Rhombic-conical net (red) as offset of a rhombic net with planar knots (yellow). The normals (black) have uniform length.

As stated pseudospheres have constant negative Gaussian curvatures, so we can expect to find a discrete analogy of Gaussian curvature for rhombic meshes with planar knots that is constantly negative as well. We will show several ways of defining such discrete curvatures which work for rhombic-conical meshes too. The results of this are at the end of section (1).

Quadrilateral nets have started to be frequently used in architecture. Rhombic meshes appear promising in that respect as with them all the edge parts can be identical. Section (3) will show ways of realizing both rhombic-conical meshes and general rhombic meshes (as constructed by approximation in section (2)) as architectural lattices.

1 Rhombic nets with planar and conical knots

1.1 Rhombic nets with planar knots

1.1.1 General definitions

These definitions will be in use throughout this thesis.

We will always deal with $\mathbb{R}^3$. The object of study will be *nets*, that is functions $f\colon \mathbb{Z}^2 \to \mathbb{R}^3$. The values $f(i,j)$, $i,j \in \mathbb{Z}$ will be called *knots* of the net. We will interchangeably use function notation $(f(i,j))$ and sequence notation (f_{ij}).

Two knots are *adjacent* if they are of the form $f(i,j)$,$f(i+1,j)$ or $f(i,j)$, $f(i,j+1)$. In this case the segment connecting them is called an *edge* of the net.

A quadruple of index pairs of the form $\big((i,j),(i,j+1),(i+1,j+1),(i+1,j)\big)$ is called a *combinatorical face* and $\big(f(i,j),f(i,j+1),f(i+1,j+1),f(i+1)\big)$ a *face* or *quadrilateral* of f. In most cases the four knots forming a face will not have a common plane in $\mathbb{R}^3$.

As mentioned, nets will have domain $\mathbb{Z}^2$, but generally results will be analogously true for functions $\{1,\dots,N\}\times\{1,\dots,M\}\to\mathbb{R}^3$, except for occasional special considerations concerning edge and corner knots. We will be calling these *finite nets*. The computer algorithms in this thesis can obviously only deal with finite nets.

To facilitate simpler notation the following functions will be used a lot:

- Operations on nets are understood pointwise, e.g. $(f+g)(i,j) := f(i,j) + g(i,j)$, $(f\times g)(i,j) := f(i,j)\times g(i,j)$, etc.
- The *shift* operator
$$(\tau_1 f)(i,j) := f(i+1,j) \quad \text{resp.} \quad (\tau_2 f)(i,j) := f(i,j+1). \tag{1}$$
Occasionally negative shifts will be used as well, namely
$$(\tau_{-1} f)(i,j) := f(i-1,j) \quad \text{resp.} \quad (\tau_{-2} f)(i,j) := f(i,j-1).$$
- The *difference* operator
$$\delta_k f := \tau_k f - f \quad \text{with } k = 1,2,-1,-2 \tag{2}$$
- The (canonical) dot product of $f,g\in\mathbb{R}^3$ will be written $\langle f,g\rangle$.
- Vectors $\in\mathbb{R}^3$ are written as columns.
$$e_1 := \left(\begin{smallmatrix}1\\0\\0\end{smallmatrix}\right),\quad e_2 := \left(\begin{smallmatrix}0\\1\\0\end{smallmatrix}\right),\quad e_3 := \left(\begin{smallmatrix}0\\0\\1\end{smallmatrix}\right) \tag{3}$$
We fix functions x, y, $z\colon \mathbb{R}^3\to\mathbb{R}$ that retrieve the first, second and third components of a vector, respectively. For example $x(f) = \langle f, e_1\rangle$.
- Rotations in $\mathbb{R}^3$ around a given axis will be used frequently too. We will denote them by rot^v_ϕ, where v is the axis and ϕ is the rotation angle (in positive direction around v). Formally rotations are multiplications with

rotation matrices. Let M be an orthonormal matrix, whose first column is $\propto v$, then

$$\mathrm{rot}^v_\phi = M \cdot \begin{pmatrix} 1 & 0 & 0 \\ 0 & \cos\phi & -\sin\phi \\ 0 & \sin\phi & \cos\phi \end{pmatrix} \cdot M^{-1}.$$

1.1.2 Rhombic nets with planar knots

In the following f will always denote a *rhombic net*, that is, a net that satisfies

$$\|\delta_1 f(i,j)\| = \|\delta_2 f(i,j)\| =: l > 0 \quad \forall\,(i,j) \in \mathbb{Z}^2. \tag{4}$$

We will also always assume a certain regularity property: We want all (signed) interior angles of rhombi to be in the range $(0, \pi)$, which is equivalent to

$$\langle \delta_1 f(i,j), \delta_2 f(i,j)\rangle > 0 \wedge \langle \delta_1 f(i,j), \delta_{-2} f(i,j)\rangle > 0 \quad \forall\,(i,j) \in \mathbb{Z}^2 \tag{5}$$

and also makes sure none of the face rhombi are degenerated.

The second half of this thesis will deal with general rhombic nets. Here only special classes of rhombic nets are considered.

A *rhombic net with planar knots* is a rhombic net where at each (i,j)

$$\delta_1 f,\ \delta_2 f,\ \delta_{-1} f,\ \delta_{-2} f \text{ lie in a common plane.} \tag{6}$$

If a rhombic net with planar knots has a face that is planar it follows that the whole net is planar. We call such a nets *trivial*. We will frequently require nets to be nontrivial for theorems and algorithms to work.

Rhombic nets with planar knots were studied by (W. Wunderlich 1952). We will now show some of his results.

Theorem 1.1. *There is an angle α such that the knot planes of $\tau_2 f$ are the knot planes of f, rotated around $\delta_2 f$ by α and the knot planes of $\tau_1 f$ are those of f rotated around $\delta_1 f$ by $-\alpha$.*

We call the angle α the *wrenching angle* of the net. The net

$$f'(i,j) := f(j,i) \quad \forall\,(i,j) \in \mathbb{Z}^2$$

has the wrenching angle $-\alpha$. Therefore we can always assume without loss of generality that $\alpha \geq 0$. We also define a number

$$\omega := \frac{\sin\alpha}{l} \geq 0 \tag{7}$$

called the *wrenching* of the net (as opposed to the wrenching *angle* α). Obviously $\omega = 0$ characterizes the trivial rhombic nets with planar knots.

1.1.3 Lelieuvre normal fields

(Bobenko-Suris 2008) define normal fields called *Lelieuvre normals* of a discrete A-net (net with planar knots). They are defined (in the case of a 2D net) as $n\colon \mathbb{Z}^2 \to \mathbb{R}^3$ such that

$$\delta_1 f = \tau_1 n \times n \text{ and } \delta_2 f = \tau_2 n \times n \tag{8}$$

Black-white-rescalings of n, that is, normal fields n' with

$$n'(i,j) = \lambda^{(-1)^{i+j}} n(i,j) = \begin{cases} \lambda\, n(i,j), & \text{if } i+j \text{ even} \\ \lambda^{-1} n(i,j), & \text{else} \end{cases} \tag{9}$$

for any $\lambda \in \mathbb{R}\backslash\{0\}$ are Lelieuvre normal fields as well.

Lelieuvre normal fields of A-nets have a nice property: They are T-nets — that is, they satisfy discrete Moutard equations: $\tau_1\tau_2 n - n \propto \tau_2 n - \tau_1 n$.

Rhombic nets with planar knots with $\alpha \neq 0$ are nondegenerate A-nets. Are Lelieuvre normals suited to study rhombic nets with planar knots?

We always assume that all rhombi are nondegenerate, that is, all their interior angles are $0 < \sigma < \pi$. Therefore $\delta_1 f \times \delta_2 f \neq 0$ and, obviously, $n(i,j) = \lambda_{ij}\delta_1 f \times \delta_2 f$.

We want to have Lelieuvre normals of uniform length. This is not possible for all A-nets, but rhombic nets with planar knots have $\|\tau_i n \times n\| = |\sin\alpha|\|\tau_i n\|\|n\| = \|\delta_i f\| = l$, so there is a Lelieuvre normal field with

$$\|n(i,j)\| = \left(\frac{\sin\alpha}{l}\right)^{-\frac{1}{2}}$$

Remember that $\frac{\sin\alpha}{l} = \omega$ is the *wrenching* defined in theorem (1.1). We see that there are exactly two Lelieuvre normal fields with normals of uniform length, which can be calculated as

$$n^+(i,j) = \frac{\delta_1 n \times \delta_2 n}{\|\delta_1 n \times \delta_2 n\|}\left(\frac{\sin\alpha}{l}\right)^{-\frac{1}{2}}(-1)^j \qquad \forall\,(i,j) \in \mathbb{Z}^2 \tag{10}$$

and

$$n^-(i,j) = \frac{\delta_1 n \times \delta_2 n}{\|\delta_1 n \times \delta_2 n\|}\left(\frac{\sin\alpha}{l}\right)^{-\frac{1}{2}}(-1)^{j+1} \quad \forall\,(i,j) \in \mathbb{Z}^2 \tag{11}$$

The last factors cause that

$$\langle\delta_1 n, n\rangle = \cos\alpha\|n\|^2 \quad \text{but} \quad \langle\delta_2 n, n\rangle = -\cos\alpha\|n\|^2$$

which is not what we want. This fact could be rectified by scaling the Lelieuvre normal field by a factor of $\sqrt{\omega}(-1)^{i+j}$, which is a step indeed taken by (Bobenko-Suris 2008). But it makes the definition of the normal field more complicated than equation (8), so we will not be using this formulation but rather define normals directly as shown in the following section.

1.1.4 Discrete Gauss maps

We therefore simply define a normalized normal field as

$$\boxed{n := \frac{\delta_1 f \times \delta_2 f}{\|\delta_1 f \times \delta_2 f\|}} \tag{12}$$

which at least satisfies modified Lelieuvre equations:

$$(-1)^{i+1}\omega^{-1}\delta_i f = \tau_i n \times n, \quad i = 1,2 \tag{13}$$

We will sometimes consider single rhombi in a coordinate system like the one in figure (4). We call this *symmetrical coordinates.*

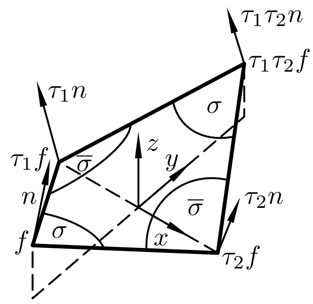

Figure 4: rhombus in symmetrical coordinates

We define the angle between adjacent edges as

$$\sigma\colon \mathbb{Z}^2 \to \mathbb{R} \quad \text{such that} \quad \langle \delta_1 f, \delta_2 \rangle = \cos\sigma \tag{14}$$

The second angle of the rhombi is called $\overline{\sigma}$. They are connected by

$$\tan\frac{\sigma}{2}\tan\frac{\overline{\sigma}}{2} = \cos\alpha$$

Rhombic nets with planar knots satisfy the following equations:

$$\begin{aligned} \tau_1 n &= \mathrm{rot}^{\delta_1 f}_{-\alpha}\, n \\ \tau_2 n &= \mathrm{rot}^{\delta_2 f}_{\alpha}\, n \end{aligned} \quad \text{and} \quad \begin{aligned} \delta_1 f &= \mathrm{rot}^{n}_{\phi}\, \delta_1 \tau_{-1} f \\ \delta_2 f &= \mathrm{rot}^{n}_{\theta}\, \delta_2 \tau_{-2} f \end{aligned} \tag{15}$$

which serve to define two further angle functions ϕ and θ, both $\mathbb{Z}^2 \to \mathbb{R}$. We get the following nomenclature for rhombic nets with planar knots:

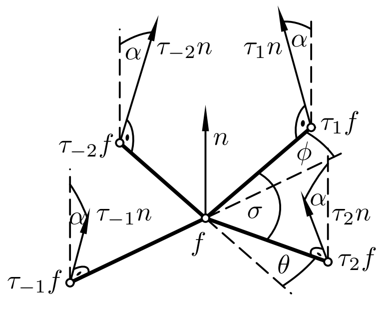

Figure 5: f and its neighborhood (at any $(i,j) \in \mathbb{Z}^2$)

The map n can be seen as a discrete version of a Gauss map of f. We find

Theorem 1.2. *Let f be a nontrivial rhombic net with planar knots. Then the discrete Gauss map n is a rhombic net.*

Proof. Equation (15) shows $\|\tau_k n - n\| = 2\sin\frac{\alpha}{2} = \text{const.},\ k = 1, 2.$ □

1.1.5 Derived conical nets

(Liu-Pottmann-Wallner-Yang-Wang 2006) introduced a type of net called a *conical net*. A two-dimensional conical net is defined as a Q-net (net with planar quadrilaterals) where for each knot exists a right circular cone cone with its tip in the knot such that the four quadrilateral planes adjacent to the knot lie tangentially to the cone. (Bobenko-Suris 2008) recommend considering conical nets as maps $\mathbb{Z}^2 \to \{\text{oriented planes in } \mathbb{R}^3\}$, which are the planes of the quadrilaterals. Using this notation we can derive a conical net h from the discrete Gauss map n of a rhombic net with planar knots by pairwise associating faces of h with edges of n.

We chose those planes that contain the appropriate edges and have normal vectors that points towards the center point of the edge.

$$\begin{aligned} h(j+i, j-i) &:= \{p \in \mathbb{R}^3 \colon \langle p - n(i,j), n(i,j) + n(i,j+1)\rangle = 0\} \text{ and} \\ h(j+i, j-i-1) &:= \{p \in \mathbb{R}^3 \colon \langle p - n(i,j), n(i,j) + n(i+1,j)\rangle = 0\} \end{aligned} \tag{16}$$

Theorem 1.3. *h, as defined above, is a conical net.*

Proof. We need to show that a quadruple of adjacent faces of h indeed has a common intersection point which is the apex of a cone, which all four faces are tangential to. Let $(p, p_2, p_{12}, p_1) := (\mathrm{Id}, \tau_2, \tau_1\tau_2, \tau_1)h(i', j')$. We discern two cases:

- $\exists\,(i,j) \in \mathbb{Z}^2 \colon (i', j') = (j+i-1, j-i-1)$: In this case each plane contains an edge of n incident with $n(i,j)$. So the planes share the point $n(i,j)$. As n is spherical and a rhombic net, its knots are all conical, that means, all the edges incident with a given knot lie on a cone with apex in $n(i,j)$. (The vector $n(i,j)$ is also the cone axis.)

- $\exists\,(i,j) \in \mathbb{Z}^2 \colon (i', j') = (j+i, j-i-1)$: The edges associated with the four faces of h form a rhombus of n, namely $(n_{ij}, n_{i,j+1}, n_{i+1,j+1}, n_{i+1,j})$. Assume w.l.o.g. $y(n_{ij} - n_{i+1,j+1}) = z(n_{ij} - n_{i+1,j+1}) = x(n_{i+1,j} - n_{i,j+1}) = 0$. Therefore the rhombus has symmetry planes $x = 0$ and $y = 0$. Then by definition the plane p is p_1 reflected across the plane $y = 0$ or p_2 reflected across $x = 0$ etc. It follows that the $p \cap p_1$ lies in the plane $y = 0$ and $p \cap p_2$ in $x = 0$. As those lines both lie in p they intersect at a point M with $x(M) = y(M) = 0$. We see $p \cap p_1 \cap p_2 \cap p_{12} = M$.

  If we fix e_3 as the cone axis we see that there is a cone with apex in M tangentially to p, and, by reasons of symmetry, to all four planes. □

1.1.6 Finite rhombic nets with planar knots

We want to show an algorithm that constructs rhombic nets with planar knots. Of course every algorithm can only have a finite number of steps, so we must constrain ourselves to finite nets.

Without loss of generality we can assume that a finite rhombic net with planar knots is a mapping

$$f \colon \{1, \dots, m_1\} \times \{1, \dots, m_2\} \to \mathbb{R}^3$$

where $\|\delta_1 f(i,j)\| = \|\delta_2 f(i', j')\| = l$, $i = 2, \dots, m_1$, $j = 1, \dots, m_2$, $i' = 1, \dots, m_1$, $j' = 2, \dots, m_2$ and the knots are all planar.

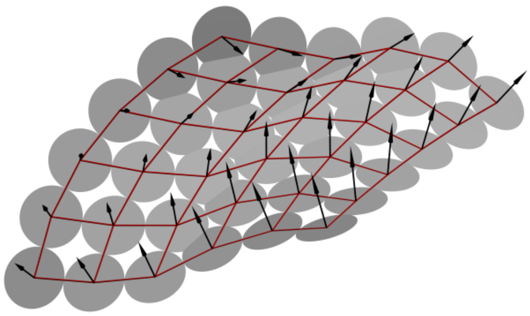

Figure 6: Rhombic net with planar knots net constructed by algorithm (1.1) with $\alpha = 0.19$.

As (W. Wunderlich 1952) noted, with rhombic nets with planar knots the fourth knot of a rhombus always follows uniquely from the first three. Based on this Wunderlich suggested two ways of specifying the shape of rhombic nets with planar knots.

- Fix one row and one column of the net, e.g. f_{i1} and f_{1j} for $i = 1, \ldots, m_1$ and $j = 1, \ldots, m_2$.
- Fix a zig-zag polygon diagonally through the net, that is f_{ij} where $i - j \in \{0, 1\}$.

We will now show an algorithm for the first approach. Algorithms for the second approach can be found similarly.

To construct the first row and column of f we will be using ϕ_{i1} and θ_{1j} via equation (15). ϕ_{i1} and θ_{1j} can be choosen freely as long as the regularity property equation (5) holds.

Algorithm 1.1. (Construction of rhombic nets with planar knots)

Input:
- (i) $\alpha \in [0, \frac{\pi}{2}), \quad l > 0$
- (ii) $\phi_{i1}, \theta_{1j}\ i = 1, \ldots, m_1,\ j = 1, \ldots, m_2$
- (iii) $f_{11}, f_{21}, f_{12} \in \mathbb{R}^3$ such that $\sigma_{11} := \arccos(l^{-2}\langle \delta_1 f_{11}, \delta_2 f_{11}\rangle \in (0, \pi)$.

$n_{11} := \delta_2 f_{11} \times \delta_1 f_{11} / \|\delta_2 f_{11} \times \delta_1 f_{11}\|$
$n_{21} := \mathrm{rot}_{-\alpha}^{\delta_1 f_{11}}\, n_{11},\ n_{11} := \mathrm{rot}_{\alpha}^{\delta_2 f_{11}}\, n_{11}$.
for i **from** 2 **to** $m_1 - 1$ **do**
  $f_{i+1,1} := f_{i1} + \mathrm{rot}_{\phi_{i1}}^{n_{i1}}\, \delta_1 f_{i1}$
  $n_{i+1,1} := \mathrm{rot}_{-\alpha}^{\delta_1 f_{i+1,1}}\, n_{i1}$
end for
for j **from** 2 **to** $m_2 - 1$ **do**
  $f_{1,j+1} := f_{1j} + \mathrm{rot}_{\theta_{1j}}^{n_{1j}}\, \delta_2 f_{1j}$
  $n_{1,j+1} := \mathrm{rot}_{\alpha}^{\delta_2 f_{1,j+1}}\, n_{1j}$
end for
for i **from** 2 **to** m_1 **do**
  for j **from** 2 **to** m_2 **do**
    $v := (n_{i-1,j} + n_{i,j-1}) \times (f_{i-1,j} - f_{i,j-1})$
    $f_{ij} := f_{i-1,j-1} + \langle \delta_2 f_{i-1,j} + \delta_1 f_{i,j-1}, v\rangle \|v\|^{-2} v$

$\qquad\qquad n_{ij} := n_{i-1,j-1} - 2\langle n_{i-1,j-1}, v\rangle \|v\|^{-2} v$

end for

end for

What choice do we have for ϕ and θ so that the algorithm will work properly? There are indeed choices that lead to violations of the regularity property, as shown by figure (7).

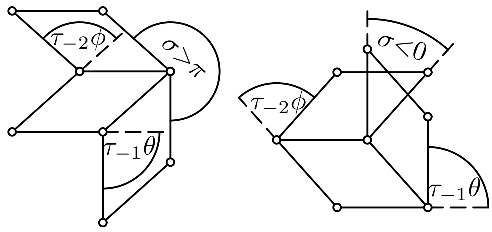

Figure 7: no possible rhombus

Theorem 1.4. *Let $(f_{ij})_{i=1,\dots,m_1,\, j=1,\dots,m_2}$ be a finite rhombic net with planar knots where $\alpha = 0$ (trivial net). Then it is possible to extend f to a finite rhombic net with planar knots $(f_{ij})_{i=1,\dots,m_1',\, j=1,\dots,m_2'}$ where $m_1' \geq m_1$ and $m_2' \geq m_2$.*

Proof. Rhombic nets with planar knots with $\alpha = 0$ are planar. Assume therefore w.l.o.g. $f\colon \{1,\dots,m_1\} \times \{1,\dots,m_2\} \to \mathbb{R}^2$.

For a row of vertices, for example $(f_{m_1,j})_{j=1,\dots,m_2}$ there exists a second row $(f_{m_1+1,j})_{j=1,\dots,m_2}$ that together with the first forms a row of rhombi if and only if

$$\forall a, b \in \{2, \dots, m_2 - 1\}\colon\; -\pi < \sum_{j=a}^{b} \theta_{ij} < \pi \tag{17}$$

holds, or, equivalently, if we can find a vector $\delta_1 f_{m_1,1} = \delta_1 f_{m_1,j},\ j = 2, \dots, m_2$ such that $\det\big(\delta_1 f_{m_1,1}, \delta_2 f_{m_1,j},\ j = 1, \dots, m_2 - 1\big) < 0$. Figure (8) illustrates this.

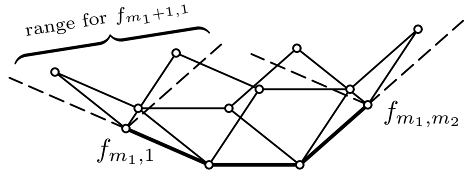

Figure 8: possible values for $f_{m_1+1,1}$

$(f_{m_1,j})_{j=1,\dots,m_2}$ does have this property, because there is a row rhombi together with $(f_{m_1-1,j})_{j=1,\dots,m_2}$. So we can construct $(f_{m_1+1,j})_{j=1,\dots,m_2}$ and increase m_1 by 1.

The same argument is used to increase m_2, and iteration proves the statement. □

For nets with $\alpha \neq 0$ (nontrivial nets) the problem is much more difficult and no answer will be given here. Still, in practice construction of rhombic nets with planar knots is possible if α, $|\phi_{i1}|$ and $|\theta_{1j}|$ are sufficiently small and σ_{00} is near $\frac{\pi}{2}$.

1.2 Rhombic nets with conical knots

We call a knot f_{ij} of a rhombic net a *conical knot*, if all vertices $(\tau_{-2}, \tau_{-1}, \tau_1, \tau_2)f_{ij}$ that are connected to f_{ij} by an edge of the net lie on a common right circular cone whose tip is at f_{ij}. The negative normalized axis of the cone is called the *normal* of the knot, which results in a function $n\colon \mathbb{Z}^2 \to \mathbb{R}^3$.

The half aperture angle of the cone is named $\widetilde{\Omega}$. We will always assume that $0 < \widetilde{\Omega} \leq \frac{\pi}{2}$, so that the cone cannot be degenerate, but will allow $\widetilde{\Omega} = \frac{\pi}{2}$, wich turns the cone into a plane. We also define a quantity Ω called the *aperture* of the cone (as opposed to the aperture *angle*) by

$$\boxed{\Omega := \cos\widetilde{\Omega} \in [0,1)}$$

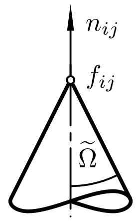

Figure 9: cone half aperture angle

This makes it easy to characterize whether a point lies on the cone:

$$p \text{ lies one the cone of the conical knot } f_{ij} \Leftrightarrow \langle p - f_{ij}, n_{ij}\rangle = -\Omega\|p - f_{ij}\|$$

We can therefore generalize equation (6): f_{ij} is a conical knot with aperture Ω if there exists a normal n_{ij} such that

$$\langle \delta_k f_{ij}, n_{ij}\rangle = -l\Omega \quad \text{for } k = -2, -1, 2, 1, \tag{18}$$

where l is the edge length of f as in the previous sections.

Is n_{ij} uniquely defined by this property? For any plane through f_{ij} which contains n_{ij} there are at most two different possibilities for knots of f adjacent to f_{ij}. Therefore there must be three neighbors of f_{ij} such that the respective edges do not lie in a plane. From this follows that equation (18) has a unique solution.

We can now attempt to define our main object of study of this chapter. We want to study rhombic nets where each vertex is a conical knot and all of them have the same aperture Ω.

Rhombic nets with planar knots can be regarded as a special case of rhombic nets with conical knots with $\Omega = 0$. As seen in theorem (1.1) the planes of adjacent knots are wrenched by a uniform angle α. We would like to reproduce this behavior with conical knots.

With conical knots there are no knot planes. Angles between planes can be defined as angles between their normal vectors. This enables us to take the angles between cone axes (conical knot normals) as a measure for the wrenching. We wish to have $\alpha \in \mathbb{R}$ such that

$$\cos\alpha \equiv \langle n, \tau_1 n\rangle, \text{ and } \cos\alpha \equiv \langle n, \tau_2 n\rangle. \tag{19}$$

Do rhombic nets with conical knots exist that do not have the property?

Unfortunately they do. In finite nets the normals of the four corner knots can generally be freely chosen from two solutions of equation (18), in particular there is always a choice so that the corner rhombus does not have the symmetry property. Also nets that consist of a single row of rhombi can have any configuration of knot normal orientations. Examples such as these could be dealt with by demanding, for example, that rhombic nets need to have at least three rows and columns of knots.

But even rhombic nets $\mathbb{Z}^2 \to \mathbb{R}^3$ can be constructed where some rhombi do not have the property, like figure (10).

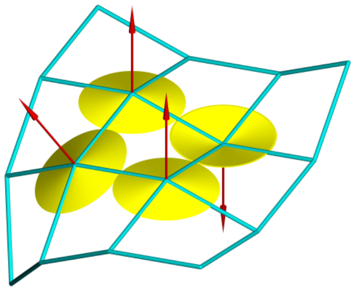

Figure 10: conical knot net without constant α — detail

We remedy this situation by simply assuming the existence of such an α.

Let $\alpha \in (-\pi, \pi]$. We can always assume $\alpha \geq 0$, as the nets with $\alpha < 0$ can be derived from those with $\alpha > 0$ by reflecting them across any plane in $\mathbb{R}^3$, which retains the value of Ω.

Therefore we arrive at the following definition:

Definition 1.1. *A* rhombic net with conical knots of uniform aperture *is a rhombic net with edge length l as defined in section (1.1.2) (equation (4)) together with a quantity $\Omega \in [0, 1)$ such that*

1. $\exists\, n\colon \mathbb{Z}^2 \to \mathbb{R}^3$ *such that*
$$\langle \delta_k f, n\rangle \equiv -l\Omega \quad \textit{for } k = -2, -1, 2, 1$$
2. $\exists\, \alpha \in [0, \pi]\colon \langle n, \tau_1 n\rangle \equiv \cos\alpha$ *and* $\langle n, \tau_2 n\rangle \equiv \cos\alpha$.
3. $\det\big(\delta_2 f(i,j), \delta_1 f(i,j), n(i,j)\big) > 0\ \forall\, (i,j) \in \mathbb{Z}^2$ *(Regularity property, analogous to equation (5))*

In this case we let $\omega := \frac{\sin\alpha}{l}$ just as with rhombic nets with planar knots.

Definition 1.2. *We will call a rhombic net with conical knots of uniform aperture with $\alpha \in [0, \frac{\pi}{2})$ a* regular rhombic-conical net*, or, in short, a* rhombic-conical net*. A net with $\alpha \in (0, \frac{\pi}{2}]$ will be called an* alternating rhombic-conical net*.*

f is rhombic net with conical knots of aperture Ω and wrenching angle $\alpha \in [0, \pi]$.
$$\rightsquigarrow \boxed{\begin{cases} \alpha \in [0, \frac{\pi}{2}) & \ldots \text{ (regular) rhombic-conical net} \\ \alpha = \frac{\pi}{2} & \ldots \text{ special case} \\ \alpha \in (\frac{\pi}{2}, \pi] & \ldots \text{ alternating rhombic-conical net} \end{cases}} \tag{20}$$

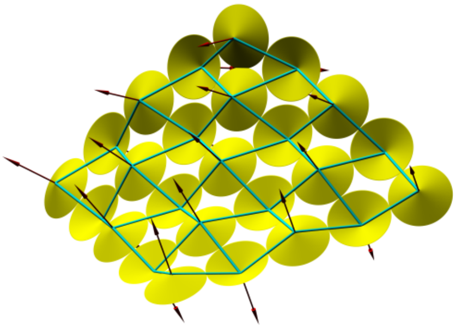

Figure 11: Alternating rhombic-conical net

Note that the notion of a rhombic-conical net is completely different from the conical nets as studied by (Liu-Pottmann-Wallner-Yang-Wang 2006) (see section (1.1.5)). Still, section (1.3.3) will show a way to associate rhombic-conical nets with certain conical nets.

Do rhombic nets with conical knots of uniform aperture with $\alpha = \frac{\pi}{2}$ exist? Yes, they do, but do not form interesting surfaces as the values of their knots form periodic sequences. Figure (12) shows an example of such a net — it has 8×8 knots, but most of them coincide.

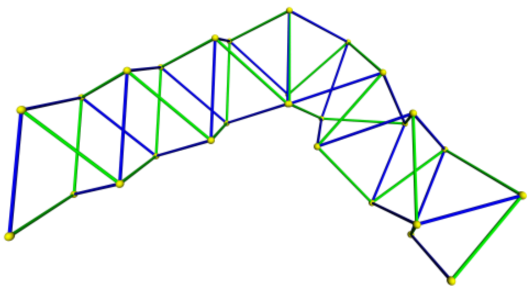

Figure 12: Net with $\alpha = \frac{\pi}{2}$, rows=blue, columns=green

In the following only regular and alternating rhombic-conical nets are studied.

In particular we find that every rhombic net with planar knots is a rhombic-conical net with $\Omega = 0$.

Theorem 1.5. *For a regular rhombic-conical net*

$$\Omega \leq \sin \frac{\alpha}{2} \tag{21}$$

always holds.

Proof. Let (p, p') be an edge of such a net and (q, q') the respective normals. Assume w.l.o.g. $p = 0$, $p' = le_1$ and $y(q) = 0$. The condition equation (18) makes sure that $-x(q) = x(q') = \Omega$. Therefore

$$q = \begin{pmatrix} -\Omega \\ 0 \\ \sqrt{1-\Omega^2} \end{pmatrix} \quad \text{and} \quad q' = \mathrm{rot}_\beta^{e_1} \begin{pmatrix} \Omega \\ 0 \\ \sqrt{1-\Omega^2} \end{pmatrix}$$

for some angle $\beta < \frac{\pi}{2}$. We calculate $\langle q, q' \rangle = -\Omega^2 + (1-\Omega^2)\cos\beta = \cos\alpha$. This can be rearranged as $\Omega^2 = 1 - \frac{1+\cos\alpha}{1+\cos\beta}$. As $\Omega \geq 0$ and $\cos\alpha > 0$ we can maximize this expression by setting $\cos\beta$ to its maximum value. Thus

$$\Omega^2 \leq 1 - \frac{1+\cos\alpha}{2} \Rightarrow \Omega = \sqrt{\frac{1-\cos\alpha}{2}} = \sin\frac{\alpha}{2} \qquad \square$$

1.3 Rhombic-conical nets as offsets

Definition 1.3. *Let $f\colon I \times J \mapsto \mathbb{R}^3$ be a net with normals $n\colon I \times J \mapsto \mathbb{R}^3$, where I and J are intervals in $\mathbb{Z}$, in which $-\infty$ and ∞ are allowed as interval borders too. The normals observe $\|n(i,j)\| = 1\ \forall\,(i,j) \in I \times J$ but are otherwise free.*

For some $\varepsilon \in \mathbb{R}$ the offset *of f (strictly speaking, of f and n, but usually it is clear which function n is meant) with distance ε is the function*

$$f'\colon I \times J \mapsto \mathbb{R}^3,\ (i,j) \mapsto f(i,j) + \varepsilon n(i,j). \tag{22}$$

The alternating offset *of f is the function*

$$f''\colon I \times J \mapsto \mathbb{R}^3,\ (i,j) \mapsto f(i,j) + (-1)^{i+j}\varepsilon n(i,j) \tag{23}$$

Offset and alternating offset nets obtain normals in a natural way. With regular offsets we simply use $n' := n$, and for alternating offsets we use

$$n''(i,j) := (-1)^{i+j} n(i,j). \tag{24}$$

Usually in offsets f will be $\mathbb{Z}^2 \mapsto \mathbb{R}^3$ and a rhombic net with planar knots, but we keep the definition more general to be able to consider offsets of single edges (e.g. $I \times J = \{i, i+1\} \times \{j\}$) in a simple way as well.

Likewise offsets of degenerated nets (e.g. ran f being a single point) are useful too sometimes.

(W. Wunderlich 1952) noted that offsets of rhombic nets with planar knots are always rhombic-conical nets. The following theorem retraces Wunderlich's argument and extends it to alternating offsets as well.

Theorem 1.6. *Let f be a rhombic net with planar knots. Then for all $\varepsilon \in [0,\infty)$ the offset of f with distance ε is a rhombic-conical net and the alternating offset of f with distance ε is an alternating rhombic-conical net.*

Proof. Let $(p_1, p_2) := (f(i,j), f(i+1,j))$ be an edge of f and the respective normals $(q_1, q_2) := (n(i,j), n(i+1,j))$. We can without loss of generality assume that $p_1 = 0$, $p_2 = le_1$ and $q_1 = e_3$. It follows $q_2 = \begin{pmatrix} 0 \\ \sin\alpha \\ \cos\alpha \end{pmatrix}$.

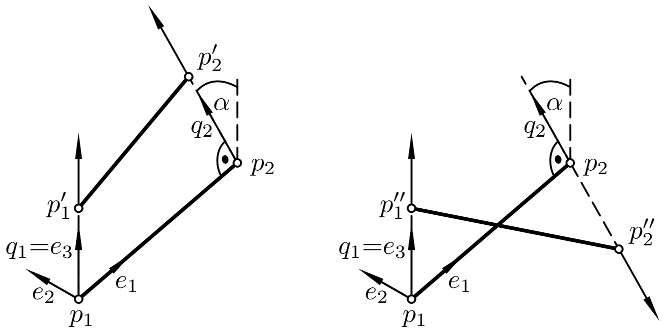

Figure 13: regular and alternating offsets

We will consider the cases of regular and alternating offsets at the same time. We can w.l.o.g. assume $i + j \equiv 0 \pmod 2$ because if not, we can simply replace ε by $-\varepsilon$.

$$p_1' := p_1'' := p_1 + \varepsilon q_1 = \begin{pmatrix} 0 \\ 0 \\ \varepsilon \end{pmatrix}, \quad p_2' := p_2 + \varepsilon q_2 = \begin{pmatrix} l \\ \varepsilon \sin\alpha \\ \varepsilon\cos\alpha \end{pmatrix}, \; p_2'' := p_2 - \varepsilon q_2$$

The length of the new edge is $l' := \|p_2' - p_1'\| = \sqrt{l^2 + (\varepsilon 2 \sin\frac{\alpha}{2})^2}$ and $l'' := \|p_2'' - p_1''\| = \sqrt{l^2 + (\varepsilon 2\cos\frac{\alpha}{2})^2}$. The normals of the new nets are, as per definition (1.3), $n' := n$ resp. $n''(i,j) := (-1)^{i+j} n(i,j)$.

$$\langle q_1, p_2' - p_1' \rangle {l'}^{-1} = -\frac{\varepsilon 2 \sin^2\frac{\alpha}{2}}{l'} \quad \text{and} \quad \langle q_1, p_2'' - p_1'' \rangle {l''}^{-1} = -\frac{\varepsilon 2\cos^2\frac{\alpha}{2}}{l''}$$

At the other end of the edge ($\langle q_2, p_1' - p_2' \rangle {l'}^{-1}$ resp. $\langle -q_2, p_1'' - p_2'' \rangle {l''}^{-1}$) we get the same results. We define

$$\Omega' := \frac{\varepsilon 2\sin^2\frac{\alpha}{2}}{\sqrt{l^2 + (\varepsilon 2\sin\frac{\alpha}{2})^2}} \quad \text{and} \quad \Omega'' := \frac{\varepsilon 2\cos^2\frac{\alpha}{2}}{\sqrt{l^2 + (\varepsilon 2\cos\frac{\alpha}{2})^2}} \tag{25}$$

If we perform all these calculation for an edge of the form $(f(i,j), f(i,j+1))$ we find the same results. The are are therefore common to all edges/knots of the offset net. With equation (18) we see that the offset nets are both rhombic-conical nets with cone apertures Ω' resp. Ω''. The first one retains the wrenching angle of the planar knots net f, $\alpha < \frac{\pi}{2}$, and is, by definition (1.2), a regular rhombic-conical net. The second one attains, by the flipping of every alternate normal the wrenching angle $\pi - \alpha > \frac{\pi}{2}$ and is therefore an alternating rhombic-conical net. $\square$

Now that we have shown that offsets of rhombic nets with planar knots are rhombic-conical nets, it suggest itself to examine, whether all rhombic-conical nets can be constructed that way.

First we will show two trivial lemmata, that will help in the next proof.

Lemma 1. *For the offsets $f + \varepsilon n$ of a rhombic net with planar knots the mapping $\varepsilon \mapsto \Omega'$ as per equation (25) is injective, provided that $\alpha \neq 0$. For alternating offsets $\varepsilon \mapsto \Omega''$ is injective for all $\alpha \in [0, \frac{\pi}{2})$.*

Proof. Assume that ε and ε' result in the same Ω'.

$$\frac{\varepsilon 2\sin^2\frac{\alpha}{2}}{\sqrt{l^2+(\varepsilon 2\sin\frac{\alpha}{2})^2}} = \frac{\varepsilon' 2\sin^2\frac{\alpha}{2}}{\sqrt{l^2+(\varepsilon' 2\sin\frac{\alpha}{2})^2}} \Rightarrow \big(l^2+(\varepsilon' 2\sin\tfrac{\alpha}{2})^2\big)\varepsilon^2 =$$
$$= \big(l^2+(\varepsilon 2\sin\tfrac{\alpha}{2})^2\big)\varepsilon'^2 \Rightarrow l^2(\varepsilon^2-\varepsilon'^2)=0 \Rightarrow \varepsilon=\varepsilon' \wedge \varepsilon=-\varepsilon'$$

$\varepsilon=-\varepsilon'$ would neccessiate $\varepsilon=\varepsilon'=0$, so $\varepsilon=\varepsilon'$ holds in any case.

For alternating offsets the procedure is the same, except that $\cos\frac{\alpha}{2}\neq 0\ \forall\alpha\in[0,\frac{\pi}{2})$. □

Lemma 2. *Let (p_1,p_2) be an edge of a net with planar knots with respective normals q_1 and q_2 with wrenching angle $\alpha\neq\pi$. ($p_1=p_2$ is allowed). Two points $p_1+\varepsilon q_1$ and $p_2+\varepsilon' q_2$ can be only be adjacent conical knots of equal aperture with normals q_1 resp. q_2 if $\varepsilon=\varepsilon'$.*

Proof.

$$\langle(p_2+\varepsilon' q_2)-(p_1+\varepsilon q_1),q_1\rangle = \langle(p_1+\varepsilon q_1)-(p_2+\varepsilon' q_2),q_2\rangle \Leftrightarrow$$
$$\Leftrightarrow \varepsilon'\langle q_2,q_1\rangle - \varepsilon\|q_1\|^2 = \varepsilon\langle q_1,q_2\rangle-\varepsilon'\|q_2\|^2 \Leftrightarrow \varepsilon'(1+\cos\alpha)=\varepsilon(1+\cos\alpha) \underset{\underset{\alpha\neq\pi}{\uparrow}}{\Leftrightarrow} \varepsilon=\varepsilon'$$
□

Let f be a (regular) rhombic-conical net. If $\alpha=0$, equation (21) allows only $\Omega=0$. Therefore f already *is* a rhomic net with planar knots. Assume therefore $\alpha>0$.

Theorem 1.7. *Let f be a regular rhombic-conical net with $\alpha\neq 0$. Then for $\Omega=\sin\frac{\alpha}{2}$ f is spheric, that is, all its knots lie on some sphere $\subset\mathbb{R}^3$, and for $\Omega<\sin\frac{\alpha}{2}$ f is an offset of a rhombic net with conical knots.*

Proof. Let $h:=f+\mathbb{R}n$ be the lines through the knots of f in the directions of n.

$h(i,j)$ and $h(i,i+1)$ are not parallel because $\alpha\neq 0$. If they are skew there is a unique segment that is perpendicular to both of them. Call that segment (p_1,p_2). If they are not skew, they have an intersection point, call it s. In this case, let $p_1:=p_2:=s$. So in any case we get

$$p_1\in h(i,j)\wedge p_2\in h(i+1,j)\wedge\langle n(i,j),p_2-p_1\rangle=\langle n(i+1,j),p_1-p_2\rangle=0$$

We can consider (p_1,p_2) to be two planar knots with normals $n(i,j)$ and $n(i+1,j)$ connected by an edge (which might not have length >0).

From this, lemma (2) shows $\|f(i,j)-p_1\|=\|f(i+1,j)-p_2\|$, so there is an $\varepsilon\in\mathbb{R}$ such that $(f(i,j),f(i+1,j))=(p_1,p_2)+\varepsilon\cdot(n(i,j),n(i+1,j))$. Solving equation (25) for ε provides a ε whose offset results in the correct value for Ω: $\varepsilon=\Omega l(2\sin^2\frac{\alpha}{2})^{-1}$.

By lemma (1) $\varepsilon\mapsto\Omega$ is injective, so it must be the required ε.

Again this is true for all edges of f and so we find that

$$f':=f-\frac{\Omega l}{2\sin^2\frac{\alpha}{2}}n \tag{26}$$

is a net with $\delta_k f' \perp n$ and $\|\delta_k f'\| = \text{const.}$, $k = 1, 2$. It is a rhombic net with planar knots if and only if $\|\delta_1 f'(i,j)\| \neq 0$ for some $(i,j) \in \mathbb{Z}^2$.

Theorem (1.6) gives the edge length of offset nets as

$$l^2 = \|\delta_k f'(i,j)\|^2 + (\varepsilon 2 \sin\frac{\alpha}{2})^2 \Rightarrow \|\delta_1 f'(i,j)\| = l^2 - \frac{\Omega^2 l^2}{\sin^2\frac{\alpha}{2}}$$

This is 0 exactly for $\Omega^2 = \sin^2\frac{\alpha}{2}$, which is, as $\Omega \geq 0$ and $\alpha > 0$ equivalent to $\Omega = \sin\frac{\alpha}{2}$ and else > 0 (as $\Omega \leq \sin\frac{\alpha}{2}$ always holds). Therefore for $\Omega < \sin\frac{\alpha}{2}$ f' is a rhombic net with planar knots, of which f is an offset.

In the case $\Omega = \sin\frac{\alpha}{2}$ f' degenerates to a single point. Obviously it is the center of a sphere with radius ε, on which all of the knots of f lie. As $h(i,j) \ni f'(i,j) = f(i+1,j) \in h(i+1,j)$, it follows that all lines through knots of f along the respective normals go through the sphere center. $\square$

For alternating rhombic-conical nets the situation is simpler:

Theorem 1.8. *Let f be an alternating rhombic-conical net. Then there exists a rhombic net with planar knots f' such that f is an alternating offset of f'.*

Proof. With alternating rhombic-conical nets neighbor normals can not intersect. They are parallel ($\Leftrightarrow \alpha = \pi$) or skew. If they are skew, they are an offset of an edge with planar knots as in the last theorem. If they are parallel then they are an offset of the edge $(p - \frac{l\Omega}{2}q, p' - \frac{l\Omega}{2}q')$ which has planar knots as well. Like in the last theorem, with lemma (1) (with $\alpha' := \pi - \alpha$ in place of α) follows that the ε derived by solving equation (25) is the correct solution. We don't have to exclude the case $\alpha' = 0$, as $\cos\frac{\alpha'}{2} \neq 0$ for $\alpha' = 0$. We find

$$f' := f - \frac{\Omega l}{2\cos^2\frac{\alpha'}{2}} n \quad \text{and} \quad n'(i,j) := (-1)^{i+j} n(i,j) \tag{27}$$

where n' are the normals of f'. The other difference to the last theorem is, that when we calculate the edge lengths of f', we find the condition

$$\Omega = \cos\frac{\alpha'}{2} \quad \Leftrightarrow \quad \|\delta_k f'\| = 0 \text{ for } k = 1, 2$$

We know $\alpha' \in [0, \frac{\pi}{2})$ and so equation (21) shows $\Omega \leq \sin\frac{\alpha'}{2} < \cos\frac{\alpha'}{2}$ and so $\|\delta_k f(i,j)\| \neq 0$. Therefore f' is a well-defined rhombic net with planar knots in every case. $\square$

1.3.1 Regularity issues

The previous section did not ask the question whether the nets that are constructed as offsets observe any regularity properties. We will now make good for this.

For rhombic nets with planar knots we have declared the regularity property equation (5):

$$0 < \sigma, \overline{\sigma} < \pi$$

As σ and $\overline{\sigma}$ are connected by

$$\tan\frac{\sigma}{2}\tan\frac{\overline{\sigma}}{2} = \cos\alpha > 0$$

we see

$$\sigma \in (0,\pi) \quad \Leftrightarrow \quad \overline{\sigma} \in (0,\pi).$$

So our regularity property simplifies to

$$\det\big(\delta_2 f, \delta_1 f, n\big) > 0. \tag{28}$$

Let's consider a rhombus of f in symmetric coordinates. In analogy to σ we define the inside angle of the offset rhombus σ'. Here $\delta_1(f+\varepsilon n) = \mathrm{rot}^n_{\sigma'}\,\delta_2(f+\varepsilon n)$ does *not* hold but still we have $\delta_1(f+\varepsilon n) = \delta_2(f+\varepsilon n) \Leftrightarrow \sigma' = 0$. For a rhombic-conical net we demand the regularity property

$$\sigma', \overline{\sigma}' > 0 \text{ everywhere.} \tag{29}$$

If we explicitly calculate f and n in symmetric coordinates we quickly find $(f+\varepsilon n)_{i+1,j} = (f+\varepsilon n)_{i,j+1}$ for $\varepsilon = \omega^{-1}\cos\alpha\cot\sigma_{ij}$. We therefore change theorem (1.6) to

Theorem 1.9. *Let f be a rhombic net with planar knots. Then for all $\varepsilon \in [0,\infty)$ the offset of f with distance ε is a rhombic-conical net which satisfies the regularity property if and only if*

$$\varepsilon < \omega^{-1}\cos\alpha\sigma(i,j)\ \forall\,(i,j) \in \mathbb{Z}^2 \tag{30}$$

The angles σ' satisfy

$$l'^2\cos\sigma' = \langle\delta_2(f+\varepsilon n), \delta_1(f+\varepsilon n)\rangle. \tag{31}$$

It is clear that for fixed offset distance $\varepsilon \geq 0$ the mapping $\sigma_{ij} \mapsto \sigma'_{ij}$ is monotonous near 0.

Assume that the rhombus is the border case $\sigma_{ij} = 0$. The we see

$$\begin{gathered} f = \begin{pmatrix} 0 \\ -l \\ 0 \end{pmatrix},\ f_{12} = \begin{pmatrix} 0 \\ l \\ 0 \end{pmatrix},\ f_1 = f_2 = 0, \\ n_{ij} = n_{i+1,j+1} = e_2,\ n_{i+1,j} = \begin{pmatrix} -\sin\alpha \\ 0 \\ \cos\alpha \end{pmatrix} \text{ and } n_{i,j+1} = \begin{pmatrix} \sin\alpha \\ 0 \\ \cos\alpha \end{pmatrix} \end{gathered} \tag{32}$$

Using the results from theorem (1.6) about l' and Ω resulting from ε

$$l' = \sqrt{l^2 + (2\varepsilon\sin\tfrac{\alpha}{2})^2} \quad \text{and} \quad \Omega = 2\varepsilon\sin^2\tfrac{\alpha}{2}l'^{-1}$$

and the values of f and n as above we can calculate the corresponding σ_{ij}. Together with the monotony we find (after some trigonometric rearranging)

$$\sigma > 0 \quad \Leftrightarrow \quad \sin\frac{\sigma'}{2} > \Omega\cot\frac{\alpha}{2} \tag{33}$$

This means that theorem (1.7) must be changed to:

Theorem 1.10. *Let f be a regular rhombic-conical net with $\Omega < \sin\frac{\alpha}{2}$. Then it is an offset of a rhombic net with conical knots that satisfies the regularity property if and only if*

$$\sin\sigma'(i,j), \sin\overline{\sigma}'(i,j) > \Omega\cot\tfrac{\alpha}{2}\ \forall\,(i,j) \in \mathbb{Z}^2 \tag{34}$$

.

1.3.2 Finite rhombic-conical nets

Rhombic-conical nets satisfy equations similar to rhombic nets with planar knots (equation (15)). These can be deduced relatively easy by purely geometric means. But we will show in the following how they can be found using only equation (15) and the fact that f is the offset of a rhombic net with planar knots f':

$$\begin{aligned}\delta_1 f = \delta(f' + \varepsilon n) = \delta_1 f' + \varepsilon\delta_1 n &\underset{\substack{\uparrow \\ \text{eq. (15)}}}{=} \operatorname{rot}^n_\phi \delta_1\tau_{-1} f' + \varepsilon\delta_1 n = \\ &= \operatorname{rot}^n_\phi \delta_1\tau_1 f - \varepsilon(\operatorname{rot}^n_\phi \delta_1\tau_{-1} - \delta_1)n\end{aligned}$$

For the bracket we first use that $\operatorname{rot}^n_\phi n = n$. Equation (15) states $\tau_1 n = \operatorname{rot}^{\delta_1 f'}_{-\alpha} n$ which is transformed to $\tau_{-1} n = \operatorname{rot}^{\delta_1\tau_{-1}f'}_{\alpha} n$. We see

$$(\operatorname{rot}^n_\phi \delta_1\tau_{-1} - \delta_1)n = (2\mathrm{Id} - \operatorname{rot}^{\delta_1 f'}_{-\alpha} - \operatorname{rot}^n_\phi \operatorname{rot}^{\delta_1\tau_{-1}f'}_{\alpha})n.$$

Next we use a general law for rotations:

$$\operatorname{rot}^w_\gamma \operatorname{rot}^v_\beta = \operatorname{rot}^{\operatorname{rot}^w_\gamma v}_\beta \operatorname{rot}^w_\gamma \tag{35}$$

which simplifies the bracket to

$$\big(2\mathrm{Id} - \operatorname{rot}^{\delta_1 f'}_{-\alpha} + \operatorname{rot}^{\operatorname{rot}^n_\phi \delta_1\tau_{-1}f'}_{\alpha} \operatorname{rot}^n_\phi\big)n \underset{\substack{\uparrow \\ \operatorname{rot}^n_\phi \delta_1\tau_{-1}f' = \delta_1 f'}}{=} \big(2\mathrm{Id} - \operatorname{rot}^{\delta_1 f'}_{-\alpha} - \operatorname{rot}^{\delta_1 f'}_{\alpha}\big)n$$

f' has planar knots, which means $\delta_1 f' \perp n$. So we get $\operatorname{rot}^{\delta_1 f'}_{-\alpha} n + \operatorname{rot}^{\delta_1 f'}_{\alpha} n = 2\cos\alpha$. This leads to

$$\delta_1 f = \operatorname{rot}^n_\phi \delta_1\tau_{-1} f - 2\varepsilon(1-\cos\alpha)n = \operatorname{rot}^n_\phi \delta_1\tau_{-1} f - 4\varepsilon \sin\tfrac{\alpha}{2}$$

Finally we employ equation (25), which gives the edge lengths and Ω for offset nets. We see

$$\begin{aligned}\delta_1 f &= \operatorname{rot}^n_\phi \delta_1\tau_{-1} f - 2l\Omega n \quad \text{and, analogously} \\ \delta_2 f &= \operatorname{rot}^n_\theta \delta_2\tau_{-2} f - 2l\Omega n.\end{aligned} \tag{36}$$

The equations for n are harder to find by these means so we will derive them geometrically (see figure (14)). The calculations are skipped here but the results are

$$\begin{aligned}\tau_1 n &= \operatorname{rot}^{\delta_1 f}_{-\overline{\alpha}} n + 2\Omega l^{-1}\delta_1 f \\ \tau_2 n &= \operatorname{rot}^{\delta_2 f}_{\overline{\alpha}} n + 2\Omega l^{-1}\delta_2 f\end{aligned} \quad \text{where} \quad \overline{\alpha} = \arccos\frac{\cos\alpha + \Omega^2}{1-\Omega^2}. \tag{37}$$

Now we can use these equations to give a modified version of algorithm (1.1) which constructs rhombic-conical nets without explicitly viewing them as offsets.

Algorithm 1.2. (Construction of rhombic-conical nets)

1: *Input:*
(i) $\alpha \in [0, \frac{\pi}{2})$, $\quad l > 0$, $\quad \Omega \in [0, 1)$

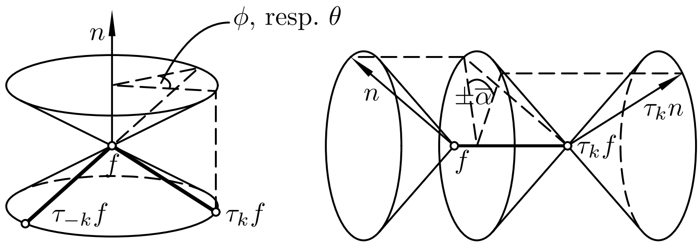

(a) Equation (36)

(b) Equation (37)

Figure 14: Equations for rhombic-conical nets at (i,j), $k = 1,2$

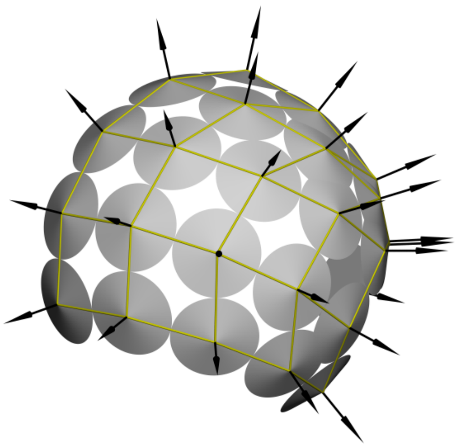

Figure 15: Rhombic-conical net constructed by algorithm (1.2) with $\Omega = 0.3$ and $\alpha = 0.19$.

(ii) ϕ_{i1}, θ_{1j} $i = 1,\dots,m_1,\ j = 1,\dots,m_2$

(iii) $f_{11}, f_{21}, f_{12} \in \mathbb{R}^3$ such that $\sigma_{11} := \arccos(l^{-2}\langle\delta_1 f_{11}, \delta_2 f_{11}\rangle \in (0,\pi)$.

$$n_{11} := -\frac{\Omega l(\delta_1 f_{11} + \delta_2 f_{11})}{l^2 + \langle\delta_1 f_{11}, \delta_2 f_{11}\rangle} + \sqrt{1 - \frac{2\Omega^2 l^2}{l^2 + \langle\delta_1 f_{11}, \delta_2 f_{11}\rangle}}\,\frac{\delta_1 f_{11} \times \delta_2 f_{11}}{\|\delta_1 f_{11} \times \delta_2 f_{11}\|}$$

$\overline{\alpha} := \arccos\big((\cos\alpha + \Omega^2)/(1-\Omega^2)\big)$

$n_{21} := \mathrm{rot}_{-\overline{\alpha}}^{\delta_1 f_{21}}\, n_{11} + 2\Omega l^{-1}\delta_1 f_{11}, \quad n_{12} := \mathrm{rot}_{\overline{\alpha}}^{\delta_2 f_{12}}\, n_{11} + 2\Omega l^{-1}\delta_2 f_{11}.$

for i **from** 2 **to** $m_1 - 1$ **do**

  $f_{i+1,1} := f_{i1} + \mathrm{rot}_{\phi_{i1}}^{n_{i1}}\, \delta_1 f_{i-1,1} - 2\Omega l n_{i1}$

  $n_{i+1,1} := \mathrm{rot}_{-\overline{\alpha}}^{\delta_1 f_{i+1,1}}\, n_{i1} + 2\Omega l^{-1}\delta_1 f_{i1}$

end for

for j **from** 2 **to** $m_2 - 1$ **do**

  $f_{1,j+1} := f_{1j} + \mathrm{rot}_{\theta_{1j}}^{n_{1j}}\, \delta_2 f_{1,j-1} - 2\Omega l n_{1j}$

  $n_{1,j+1} := \mathrm{rot}_{\overline{\alpha}}^{\delta_2 f_{1,j+1}}\, n_{1j} + 2\Omega l^{-1}\delta_2 f_{1j}$

end for

for i **from** 2 **to** m_1 **do**

  for j **from** 2 **to** m_2 **do**

    $v := (n_{i-1,j} + n_{i,j-1}) \times (f_{i-1,j} - f_{i,j-1})$

    $f_{ij} := f_{i-1,j-1} + \langle\delta_2 f_{i-1,j} + \delta_1 f_{i,j-1}, v\rangle\|v\|^{-2} v$

```
17:         n_{ij} := n_{i-1,j-1} - 2⟨n_{i-1,j-1}, v⟩‖v‖^{-2} v
18:     end for
19: end for
```

Of course this algorithm can be used in place of algorithm (1.1), if we let $\Omega = 0$. It even makes sense from the point of view of performance: Lines 1 to 11 are basically only initialization, which takes linear time. The rest of the algorithm takes $\mathcal{O}(m_1 \cdot m_2)$ but we note that it is comletely unchanged from algorithm (1.1), so there is very little overall performance loss.

We even find that, without any adjustment we can use the algorithm to construct alternating rhombic nets as well.

1.3.3 Derived circular nets

A (two-dimensional) circular net is a Q-net (net with planar quadrilaterals) where all quadrilaterals are circular, that is, their vertices lie on a common circle.

There is a simple way to derive circular nets from rhombic-conical nets. First we fix a weight function $w\colon \mathbb{Z}^2 \to \mathbb{R}$ of the following form

$$w(i,j) = \begin{cases} \lambda, & \text{if } i+j \text{ even} \\ 1-\lambda, & \text{else} \end{cases} \quad \text{for some } 0 < \lambda < 1 \tag{38}$$

In particular $w \equiv \frac{1}{2}$ is possible. Then we can define a discrete net $g\colon \mathbb{Z}^2 \to \mathbb{R}^3$ as

$$\begin{aligned} g(j+i, j-i) &:= w(i,j)f(i,j) + w(i,j+1)f(i,j+1) \text{ and} \\ g(j+i, j-i-1) &:= w(i,j)f(i,j) + w(i+1,j)f(i+1,j) \end{aligned} \tag{39}$$

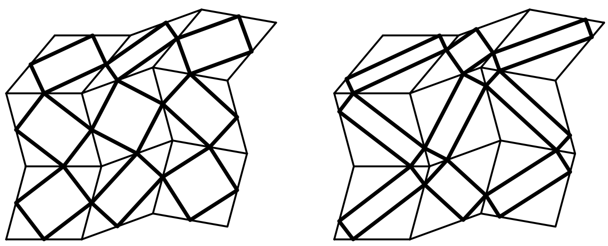

(a) $w \equiv 1/2$ (b) $w \in \{1/4, 3/4\}$

Figure 16: Derived circular nets

For every knot $f(i,j)$ there is a quadrilateral of g that “goes around” $f(i,j)$, that is, its vertices lie on the edges of f that incide with $f(i,j)$. We fix a map that gives this quadrilateral as a combinatorical face of g (a quadruple of index pairs in the order in which the edge of the quadrilateral traverses them).

$$G\colon \mathbb{Z}^2 \to (\mathbb{Z}^2)^4,\ (i,j) \mapsto (\mathrm{Id}, \tau_2, \tau_1\tau_2, \tau_1)(j+i-1, j-i-1) \tag{40}$$

Theorem 1.11. *g, as defined above, is a circular net.*

Proof. Let $g = g(i,j)$ be a knot of the net and consider the quadrilateral $Q := (g, \tau_2 g, \tau_1\tau_2 g, \tau_1 g)$.

1. $i \equiv j \pmod 2 \Rightarrow$ the knots of Q all lie on edges of f that are incident with $f\big(\frac{i-j}{2}, \frac{i+j}{2} - 1\big)$. Their distance from $f\big(\frac{i-j}{2}, \frac{i+j}{2} - 1\big)$ is uniformly $w\big(\frac{i-j}{2}, \frac{i+j}{2}\big)l$. Points on a one-sided cone that have uniform distance from the apex form a circle. Therefore Q is circular.

2. $i \not\equiv j \pmod 2 \Rightarrow$ the knots of Q lie on four different edges that form a rhombus of f, $(p, \tau_2 p, \tau_1\tau_2 p, \tau_1 p)$. $\tau_2 p$ is the knot incident with the edges of f which $\tau_2 g$ and $\tau_1\tau_2 g$ are on. $\tau_2(g, \tau_2 g, \tau_1\tau_2 g, \tau_1 g)$ is a quadrilateral of g that matches case (1). Therefore $\|\tau_2 g - \tau_2 p\| = \|\tau_1\tau_2 g - \tau_2 p\| = w\big(\frac{i-j+1}{2}, \frac{i+j+1}{2}\big)l$. In the same way we find $\|g - \tau_1 p\| = \|\tau_2 g - \tau_1 p\| = w\big(\frac{i-j+1}{2}, \frac{i+j+1}{2}\big)l$. Considering the rhombus in symmetric coordinates now makes it clear that Q is a rectangle, and obviously circular. ☐

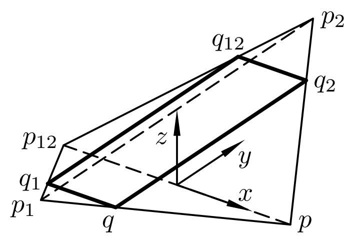

Figure 17: Theorem (1.11), case (2)

Two polyhedral surfaces are called parallel if their corresponding edges are parallel (as stated in (Bobenko-Suris 2008)).

Theorem 1.12. *Let f be a rhombic-conical net and f' an offset of it. Then the derived circular net of f, g and the one of f', g' are parallel poyhedral surfaces, even if they use different weights.*

Proof. Let (p, p_2, p_{12}, p_1) be a rhombus of f. Assume w.l.o.g. that it has symmetric coordinates. Let (q, q_2, q_{12}, q_1) be the associated quadrilateral of g as in figure (17). The normals of the rhombus are symmetric too. Therefore when we calculate the rhombus of f', $(p', p'_2, p'_{12}, p'_1)$ we find that still $y(p') = y(p'_{12}) = x(p'_1) = x(p'_2) = 0$ and $z(p'_2) = z(p'_1)$, $z(p') = z(p'_{12})$. From this obviously follows for the quadrilateral of g' that $q'_2 - q' \propto e_2 \propto q_2 - q$ and analogous for the other 3 edges. ☐

Q-nets have a natural discrete Gauss map as we can use the face normals (with appropriate orientation).

As offsets do not change the normals of rhombic nets with planar knots we can also construct derived conical nets (see section (1.1.5)) from the normals of rhombic-conical nets.

Theorem 1.13. *The discrete Gauss map of g is just the cone axes of the conical net h derived from n in section (1.1.5).*

Proof. Skipped, but is easy. ☐

The next obvious step is to characterize when a net is a circular net derived from a rhombic-conical net. We will first show the appropriate result for rhombic nets with planar knots.

We will shortly call those combinatorical faces (resp. faces) of a net of the form

$$\big(q(i,j), q(i,j+1), q(i+1,j+1), q(i+1,j)\big) \text{ for } i+j \equiv 1 \,(\mathrm{mod}\ 2) \tag{41}$$

the *white faces*, and the others the *black faces* (as in an infinite checkerboard).

Theorem 1.14. *Let $q\colon \mathbb{Z}^2 \to \mathbb{R}^3$ be a circular net. Then q is derived from a rhombic net with planar knots in the way shown above if and only if q has the following properties:*

1. *Every white face of q is rectangular.*
2. *If m_1 and m_2 are the centers of the circumcircles of two black faces that share a knot k of q, then k lies on the line through m_1 and m_2.*

Proof. The "⇒" part of the proof is clear, as the first property has already been shown and the second one follows from the construction of derived circular nets, as for rhombic nets with planar knots the knots coincide with the centers of the black faces.

Assume now that q has the properties stated above. Let p be the net of the centers of the circumcircles of the black faces of q. We can for example explicitly describe $p(i,j)$ as the center of the circle of that combinatorical face of q that is given by $G(i,j)$ (see equation (40)).

Consider two edges of p that share a knot and of which one lies in a row and the other one in a column of p. The three black faces that are used to construct the three knots of those edges all border on a common white face. Assume w.l.o.g. that that face is

$$(a,b,c,d) = \left(\begin{pmatrix} -s \\ -t \\ 0 \end{pmatrix}, \begin{pmatrix} s \\ -t \\ 0 \end{pmatrix}, \begin{pmatrix} s \\ t \\ 0 \end{pmatrix}, \begin{pmatrix} -s \\ t \\ 0 \end{pmatrix} \right).$$

Let m_1, m_2 and m_3 be these knots, being the centers of the circumcircles of the black faces through a and d, a and b and b and c, respectively (see the figure below).

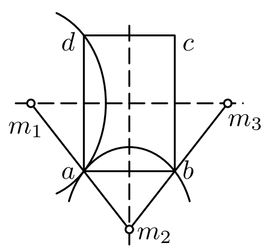

Figure 18: Proof of theorem (1.14)

Obviously for geometric reasons m_2 has to lie on the plane through $\frac{a+b}{2}$ normal to $b-a$ and therefore $x(m_2) = 0$. Likewise we see $y(m_1) = y(m_3) = 0$. By the second assumed property of q the knot a lies on the edge (m_1, m_2) and

b on (m_2, m_3). Therefore m_1 is the intersection of the line $t \mapsto m_2 + t(a - m_2)$ and the plane $y = 0$ and m_3 is the intersection of $t \mapsto m_2 + t(b - m_2)$ and the same plane. From $y(a) = y(b)$ follows that $m_1 = m_2 + t(a - m_2)$ and $m_3 = m_2 + t(b - m_2)$ for the same t. Now $x(m_2) = 0$, $x(a) = -x(b)$ and $z(a) = -z(b)$ show $x(m_1) = -x(m_3)$ and $z(m_1) = z(m_3)$. Therefore $\|m_1 - m_2\| = \|m_3 - m_2\|$.

Using this argument three times shows that all edges from each knot have the same length, and induction proves that p is a rhombic net. The fact that each knot of p is the centers of a circle and the edges originating from the knot contain a point of the circle proves that the knots of p are planar. □

Now this can be generalized in an obvious way to rhombic-conical nets.

Theorem 1.15. *Let q be a circular net whose white faces are rectangular. Let p be the net of the centers of the circumcircles of the black faces as in the previous theorem. Let n be the net of the normalized normal vectors of the planes of the circumcircles. If there is a $\lambda \in \mathbb{R}$ such that for each two black faces of q that share a knot c and the centers of the two faces $p(i,j)$ and $\tau_k p(i,j)$ ($k = 1$ or 2)*

$$\text{the edge } \big((p + \lambda n)(i,j), \tau_k(p + \lambda n)(i,j)\big) \text{ contains } c, \tag{42}$$

then $p + \lambda n$ is a rhombic-conical net that has q as a derived circular net.

Proof. Omitted, but follows easily from the theorem above. □

1.4 Discrete Gaussian curvatures

1.4.1 Shape operators for offset surfaces

For a differentiable surface $f\colon \mathbb{R}^2 \to \mathbb{R}^3$ the *Gauss map* (Gauss normals) is defined as

$$\nu\colon \mathbb{R}^2 \to \mathbb{R}^3,\ u = (u_1, u_2) \mapsto \frac{\frac{\partial f}{\partial u_1} \times \frac{\partial f}{\partial u_2}}{\left\| \frac{\partial f}{\partial u_1} \times \frac{\partial f}{\partial u_2} \right\|}. \tag{43}$$

The gradients of f and ν at u can be both seen as linear maps

$$\begin{aligned} \nabla f\big|_u &\colon T_u\mathbb{R}^2 \to T_u f \\ \nabla \nu\big|_u &\colon T_u\mathbb{R}^2 \to T_u f \end{aligned} \tag{44}$$

where $T_u\mathbb{R}^2 = \{u\} \times \mathbb{R}^2 \cong \mathbb{R}^2$ is formally the tangent space of the domain of f at u and $T_u f$ is the tangent space of f at u.

We assume that f is regular, therefore ν is well-defined everywhere which makes $\nabla f\big|_u$ an isomorphism and reversible. This enables us to define a map

$$L_u := -(\nabla \nu\big|_u) \circ (\nabla f\big|_u)^{-1}, \quad T_u f \to T_u f \tag{45}$$

called the *shape operator* of f.

The *principal directions* of a surface are the eigenvectors of its shape operators. They are the directions where the surface's (normal) curvature takes on its maximum resp. minimum value. The respective eigenvalues are called the *principal curvatures*. We will denote them by κ_1 and κ_2. They are combined to form

$$\begin{aligned} H &:= \tfrac{1}{2}(\kappa_1 + \kappa_2) && \text{mean curvature} \\ K &:= \kappa_1 \cdot \kappa_2 && \text{Gaussian curvature} \end{aligned} \tag{46}$$

To find principal curvatures we have to find $\kappa \in \mathbb{R}$ such that

$$-(\nabla\nu\big|_u) \circ (\nabla f\big|_u)^{-1} x = \kappa x \quad \text{for some } x \neq 0.$$

$\nabla f\big|_u$ is bijektive, so we let $y := \nabla f\big|_u^{-1} x$

$$\Leftrightarrow \quad -(\nabla\nu\big|_u) y = \kappa(\nabla f\big|_u) y.$$

Therefore it holds that

$$\kappa \text{ is a principal curvature of } f \quad \Leftrightarrow \quad \ker\left(\nabla\nu\big|_u + \kappa\nabla f\big|_u\right) \neq \{\vec{0}\}. \tag{47}$$

The aim of this section is to study several methods of defining and calculating Gaussian curvatures of rhombic nets with conical knots of uniform aperture. It amounts to finding suitable discrete analoga to equation (47).

Rhombic nets with conical knots of uniform aperture are, as we have seen in section (1.3), offset surfaces of rhombic nets with planar knots. A continuous offset surface is a surface $f' \colon \mathbb{R}^2 \to \mathbb{R}^3$ such that

$$\exists\, f \colon \mathbb{R}^2 \to \mathbb{R}^3 \text{ with Gauss normal } \nu \colon f' = f + \varepsilon\nu \text{ for some } \varepsilon \in \mathbb{R}$$

If we abbreviatorily write $\partial_v := \frac{\partial}{\partial v}$ the Gauss map of $f + \varepsilon\nu$ is proportional to

$$\begin{aligned} \partial_{u_1}(f + \varepsilon\nu) \times \partial_{u_2}(f + \varepsilon\nu) = \underbrace{\partial_{u_1} f \times \partial_{u_2} f}_{\propto\, \nu} &+ \varepsilon(\partial_{u_1} f \times \partial_{u_2}\nu + \\ &+ \partial_{u_1}\nu \times \partial_{u_2} f) + \varepsilon^2(\partial_{u_1}\nu \times \partial_{u_2}\nu). \end{aligned}$$

From the definition of the Gauss map follows $\partial_{u_1} f, \partial_{u_2} f \perp \nu$. Further, for all differentiable maps ν whose codomain is the unit sphere holds $\partial_{u_1}\nu, \partial_{u_2}\nu \perp \nu$. From this we can obviously infer $\partial_{u_1}\nu \times \partial_{u_2}\nu \propto \nu$ and also $\partial_{u_1} f \times \partial_{u_2}\nu \propto \nu$ and $\partial_{u_\nu} \times \partial_{u_2} f \propto \nu$. Therefore the Gauss map of $f + \varepsilon\nu$ is proportional to ν. For sufficiently small absolute values of ε their orientations match too. This means we can use ν as the Gauss map of $f + \varepsilon\nu$.

In such a case, equation (47) can be specialized as

$$\boxed{\kappa \text{ is principal curv. of } f + \varepsilon\nu \Leftrightarrow \ker\left(\kappa\nabla f\big|_u + (\kappa\varepsilon + 1)\nabla\nu\big|_u\right) \neq \{0\}.} \tag{48}$$

We will now study discrete analoga of this condition.

1.4.2 Discrete derivatives

The usual method of defining discrete derivatives is to use finite differences instead of differentials. Having in mind refinements of nets it makes sense to not consider them functions $\mathbb{Z}^2 \to \mathbb{R}^3$ but rather $(l\mathbb{Z})^2 \to \mathbb{R}^3$. In this case we have

$$\frac{\partial}{\partial u_1} f \approx \frac{f(u_1+l,u_2)-f(u1,u_2)}{(u_1+l)-u_1} = \frac{\delta_1 f}{l} \text{ and } \frac{\partial}{\partial u_2} f \approx \frac{\delta_2 f}{l} \tag{49}$$

This "normalizing" by l will have no effect on results but allows simpler notation.

For a rhombic net with planar knots the tangent space is obviously the knot plane.

Assume without loss of generality that $f(i,j)=0$, $n(i,j)=e_3$ and $\delta_1 f(i,j) = le_1$. It suggests itself that we will use n as the discrete version of ν. If we use forward differences for $\frac{\partial}{\partial u_k}\nu$ too we get

$$\frac{\partial}{\partial u_1}\nu\Big|_u \approx \frac{\delta_1 n}{l}(i,j) = l^{-1}(\operatorname{rot}_{-\alpha}^{\delta_1 f(i,j)} n - n)(i,j) = l^{-1}\left(\left(\begin{smallmatrix}0\\ \sin\alpha\\ \cos\alpha\end{smallmatrix}\right) - \left(\begin{smallmatrix}0\\0\\1\end{smallmatrix}\right)\right) = \left(\begin{smallmatrix}0\\ \omega\\ \omega\tan\frac{\alpha}{2}\end{smallmatrix}\right)$$

The problem here is that $\delta_i n/l$ does (except for degenerated nets) *not* lie in the knot plane, as $z(\delta_i n/l) = \omega \tan\frac{\alpha}{2} \neq 0$. Therefore the shape operator would not be well-defined.

The simplest way to remedy this situation is to simply change the discrete equivalent of $\frac{\partial}{\partial u_k}\nu$ so that it forces the derivatives to be in the knot plane.

$$\frac{\partial}{\partial u_k}\nu \approx \frac{\delta_k n - \langle \delta_k n, n\rangle n}{l} = \frac{\tau_k n - \langle \tau_k n, n\rangle n}{l} = \frac{\tau_k n - n\cos\alpha}{l} \tag{50}$$

which in the current situtation gives us

$$\begin{aligned} \frac{\partial}{\partial u_1}\nu\Big|_u &\approx \frac{\tau_1 n - n\cos\alpha}{l}(i,j) = \left(\begin{smallmatrix}0\\ \omega\\ 0\end{smallmatrix}\right) \text{ and} \\ \frac{\partial}{\partial u_2}\nu\Big|_u &\approx \frac{\tau_2 n - n\cos\alpha}{l}(i,j) = \operatorname{rot}_{-\sigma}^{e_3}\left(\begin{smallmatrix}0\\ -\omega\\ 0\end{smallmatrix}\right). \end{aligned} \tag{51}$$

Now we can insert this and

$$\nabla f\Big|_u \approx \left(\frac{\delta_1}{l}, \frac{\delta_2}{l}\right) f(i,j) = \left(\left(\begin{smallmatrix}1\\0\\0\end{smallmatrix}\right), \operatorname{rot}_{-\sigma}^{e_3}\left(\begin{smallmatrix}1\\0\\0\end{smallmatrix}\right)\right)$$

into equation (48) and solve for κ_1 and κ_2.

We obtain the equation

$$\Big(\kappa e_1 + \omega(\kappa\varepsilon+1)e_2,\ \operatorname{rot}_{-\sigma}^{e_3}\left(\kappa e_1 - \omega(\kappa\varepsilon+1)e_2\right)\Big) \cdot \left(\begin{smallmatrix}v_1\\ v_2\end{smallmatrix}\right) = 0$$

As $\|\kappa e_1 + \omega(\kappa\varepsilon+1)e_2\| = \|\operatorname{rot}_{-\sigma}^{e_3}(\kappa e_1 - \omega(\kappa\varepsilon+1)e_2)\|$ this is only possible for $\left(\begin{smallmatrix}v_1\\ v_2\end{smallmatrix}\right) \propto \left(\begin{smallmatrix}1\\ 1\end{smallmatrix}\right)$ or $\left(\begin{smallmatrix}-1\\ 1\end{smallmatrix}\right)$. This gives us

$$\kappa \text{ is principal curv. of } (f+\varepsilon n)(i,j) \Leftrightarrow \pm\left(\begin{smallmatrix}\kappa\\ \omega(\kappa\varepsilon+1)\\ 0\end{smallmatrix}\right) = \operatorname{rot}_{-\sigma}^{e_3}\left(\begin{smallmatrix}\kappa\\ -\omega(\kappa\varepsilon+1)\\ 0\end{smallmatrix}\right) \tag{52}$$

The first component of this equation is $\pm\kappa = \cos\sigma\,\kappa - \sin\sigma\,\omega(\kappa\varepsilon+1)$ which is solved to

$$\kappa_{1,2} = \frac{\omega}{\cot\sigma - \omega\varepsilon \mp \frac{1}{\sin\alpha}}. \tag{53}$$

It can be easily verified that these solutions are consistent with the second component of equation (52). Our final result therefore is

$$\boxed{K = \kappa_1\kappa_2 = \frac{-\omega^2}{1+2\varepsilon\omega\cot\sigma - \varepsilon^2\omega^2}.} \tag{54}$$

1.4.3 Central differences

Another method of solving the problem of $\delta_k n/l$ not lying in the tangent plane of f is the use of central differences instead of forward differences. Usually they are defined as

$$\text{central difference of } h \text{ at } t := h\big(t+\tfrac{1}{2}\big) - f\big(t-\tfrac{1}{2}\big).$$

We cannot use this definition, as f's domain is $\mathbb{Z}^2$. So instead we use

$$\delta_k^c := \frac{1}{2}(\delta_k + \delta_{-k}) = \frac{1}{2}(\tau_k - \tau_{-k}) \tag{55}$$

$$\Rightarrow \frac{\partial}{\partial u_k} f \approx \frac{\delta_k^c f}{l} = \frac{\tau_k f - \tau_{-k} f}{l} \quad \text{and} \quad \frac{\partial}{\partial u_k} n \approx \frac{\delta_k^c n}{l} = \frac{\tau_k n - \tau_{-k} n}{l}. \tag{56}$$

We assume w.l.o.g. the same coordinate system as in the last section. Using the the results of equation (15) and aided by figures (19a) and (19b) we find

$$\nabla f\big|_u \approx l^{-1}(\delta_1^c f, \delta_2^c f)(i,j) = (2l)^{-1}\big(e_1 + \mathrm{rot}^{e_3}_{-\phi}\, e_1,\ \mathrm{rot}^{e_3}_{-\sigma}(e_1 + \mathrm{rot}^{e_3}_{-\theta}\, e_1)\big) =$$
$$= \left(\cos\frac{\phi}{2}\,\mathrm{rot}^{e_3}_{-\frac{\phi}{2}}\, e_1,\ \cos\frac{\theta}{2}\,\mathrm{rot}^{e_3}_{-\sigma-\frac{\theta}{2}}\, e_1\right)$$

and

$$\nabla \nu\big|_u \approx l^{-1}(\delta_1^c n, \delta_2^c n)(i,j) =$$
$$= (2l)^{-1}\left(\left(\begin{smallmatrix}0\\ \sin\alpha\\ \cos\alpha\end{smallmatrix}\right) - \mathrm{rot}^{e_3}_{-\phi}\left(\begin{smallmatrix}0\\ -\sin\alpha\\ \cos\alpha\end{smallmatrix}\right),\ \mathrm{rot}^{e_3}_{-\sigma}\left(\left(\begin{smallmatrix}0\\ -\sin\alpha\\ \cos\alpha\end{smallmatrix}\right) - \mathrm{rot}^{e_3}_{-\theta}\left(\begin{smallmatrix}0\\ \sin\alpha\\ \cos\alpha\end{smallmatrix}\right)\right)\right) =$$
$$= \left(\omega\cos\frac{\phi}{2}\,\mathrm{rot}^{e_3}_{-\frac{\phi}{2}}\, e_2,\ -\omega\cos\frac{\phi}{2}\,\mathrm{rot}^{e_3}_{-\sigma-\frac{\theta}{2}}\, e_2\right).$$

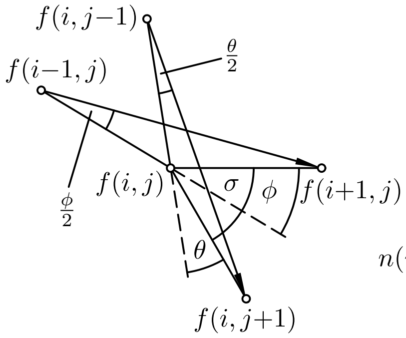

(a) central differences of f

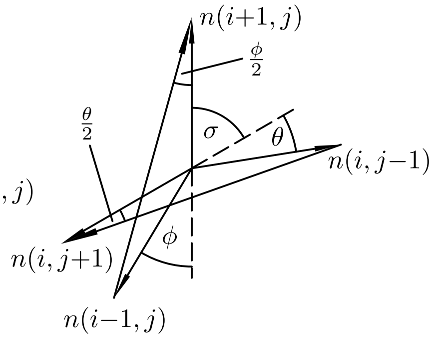

(b) central differences of n

Figure 19: central differences (length doubled)

Note that these discrete derivatives of f and n all lie in the knot plane, so the discrete shape operator is well-defined. We now can insert these results into the template equation (48) and see that κ is a principal curvature if and only if

$$\exists \left(\begin{smallmatrix}v_1\\ v_2\end{smallmatrix}\right) \neq 0\colon \left(\cos\frac{\phi}{2}\,\mathrm{rot}^{e_3}_{-\frac{\phi}{2}}\left(\begin{smallmatrix}\kappa\\ \omega(\varepsilon\kappa+1)\\ 0\end{smallmatrix}\right),\ \cos\frac{\theta}{2}\,\mathrm{rot}^{e_3}_{-\frac{\theta}{2}-\sigma}\left(\begin{smallmatrix}\kappa\\ -\omega(\varepsilon\omega-1)\\ 0\end{smallmatrix}\right)\right)\cdot\left(\begin{smallmatrix}v_1\\ v_2\end{smallmatrix}\right) = 0 \tag{57}$$

We see that $\binom{v_1}{v_2}$ must satisfy $\binom{v_1}{v_2} \propto \binom{\cos(\theta/2)}{\cos(\phi/2)}$ or $\binom{v_1}{v_2} \propto \binom{-\cos(\theta/2)}{\cos(\phi/2)}$. This leads to the equation

$$\kappa \text{ is principal curv. of } (f+\varepsilon n)(i,j) \Leftrightarrow \pm \operatorname{rot}^{e_3}_{-\frac{\phi}{2}} \begin{pmatrix} \kappa \\ \omega(\varepsilon\kappa+1) \\ 0 \end{pmatrix} = \operatorname{rot}^{e_3}_{-\sigma-\frac{\theta}{2}} \begin{pmatrix} \kappa \\ -\omega(\varepsilon\kappa+1) \\ 0 \end{pmatrix}$$

We multiply this equation with the regular matrix $\operatorname{rot}^{e_3}_{\frac{\phi}{2}}$ and obtain

$$\kappa \text{ is principal curv. of } (f+\varepsilon n)(i,j) \Leftrightarrow \pm \begin{pmatrix} \kappa \\ \omega(\varepsilon\kappa+1) \\ 0 \end{pmatrix} = \operatorname{rot}^{e_3}_{-\sigma+\frac{\phi-\theta}{2}} \begin{pmatrix} \kappa \\ -\omega(\varepsilon\kappa+1) \\ 0 \end{pmatrix} \tag{58}$$

This is exactly equation (52) with $\sigma - \frac{\phi-\theta}{2}$ instead of σ. Therefore the end result must be

$$\boxed{K = \frac{-\omega^2}{1 + 2\varepsilon\omega\cot(\sigma - \frac{\phi-\theta}{2}) - \varepsilon^2\omega^2}.} \tag{59}$$

1.4.4 Using derived circular nets

(Bobenko-Suris 2008) describe a way to define discrete curvatures for parallel Q-nets using a discrete version of Steiner's formula.

Rhombic-conical nets are only Q-nets if they are trivial, but we can make use of the derived circular nets described in section (1.3.3). This enables us to not only calculate curvatures for knots but also for the rhombi of the net.

For the derived circular net we will be using the constant weight function $w \equiv \frac{1}{2}$ for simplicity but interestingly other weights result in the same values for knot curvature.

With these weights we can easily explicate the values of the vertices of the quadrilateral of g "around" knots of f:

$$g_f \circ G = \frac{1}{2}(\mathrm{Id} + \tau_{-2}, \mathrm{Id} + \tau_{-1}, \mathrm{Id} + \tau_2, \mathrm{Id} + \tau_1)\, f \tag{60}$$

where G is the combinatorical face of g_f around $f(i,j)$ as defined in equation (40).

As we have seen in theorem (1.12) the derived circular nets of the offsets of f are parallel surfaces of g_f. They form a vector space and the family of parallel surfaces $\{g_{f+\varepsilon n} \colon \varepsilon \in \mathbb{R}\}$ can be parametrized in the form $g_{f+\varepsilon n} = g_f + \varepsilon n_g$ for some $n_g \colon \mathbb{Z}^2 \to \mathbb{R}^3$. It follows that $n_g = g_{f+n} - g_f$ is a circular net too. We see

$$n_g \circ G = (g_{f+n} - g_f) \circ G \underset{\substack{\uparrow \\ \text{equation (60)}}}{=} \frac{1}{2}(\mathrm{Id} + \tau_{-2}, \mathrm{Id} + \tau_{-1}, \mathrm{Id} + \tau_2, \mathrm{Id} + \tau_1)\, n \tag{61}$$

The normals n_g are called a *generalized Gauss map.*

For a planar quadrilateral (p_2, p_1, p_3, p_4) the oriented area of the quadrilateral $A(p_2, p_1, p_3, p_4)$ is a quadratic form and can be calculated as

$$A(p_2, p_1, p_3, p_4) = \frac{1}{2}\big([p_2, p_1] + [p_1, p_3] + [p_3, p_4] + [p_4, p_2]\big) \tag{62}$$

where $[.,.]$ is the area form of the plane of the quadrilateral. For two vectors a, b, with oriented angle γ from a to b we have $[a, b] = \|a\|\|b\| \sin\gamma$.

Now we can calculate the oriented area of the quadrilateral $n_g \circ G(i,j)$. Assume without loss of generality that $n(i,j) = e_3$, $f(i,j) = 0$ and $\tau_1 f(i,j) = le_1$.

Let $(p_{-2}, p_{-1}, p_2, p_1) := g_{f+\varepsilon n} \circ G(i,j)$ and $(q_{-2}, q_{-1}, q_2, q_1) := n_g \circ G(i,j)$.

Then from $\tau_1 n = \mathrm{rot}_{-\alpha}^{\delta_1 f}\, n$ follows $n(i+1,j) = \left(\begin{smallmatrix} 0 \\ \sin\alpha \\ \cos\alpha \end{smallmatrix}\right)$ and consequently $q_1 = \frac{1}{2}(n(i,j) + n(i+1,j)) = (0, \frac{\sin\alpha}{2}, \frac{1+\cos\alpha}{2})^T$.

Likewise we get $p_1 = \frac{1}{2}(f(i,j) + f(i+1,j)) + \varepsilon q_1 = (\frac{l}{2}, \varepsilon\frac{\sin\alpha}{2}, \varepsilon\frac{1+\cos\alpha}{2})^T$.

Analogous calculations yield $q_2 = \mathrm{rot}_{-\sigma}^{e_3}(0, -\frac{\sin\alpha}{2}, \frac{1+\cos\alpha}{2})^T$ respectivly $p_2 = \mathrm{rot}_{-\sigma}^{e_3}(\frac{l}{2}, -\varepsilon\frac{\sin\alpha}{2}, \varepsilon\frac{1+\cos\alpha}{2})^T$.

The other two normals and knots of $g_{f+\varepsilon n} \circ G(i,j)$ can be found by rotating those calculated above by appropriate angles around e_3.

All knots in $g_{f+\varepsilon n} \circ G(i,j)$ have the same z-coordinate, so the plane of $g_{f+\varepsilon n} \circ G(i,j)$ is parallel to the plane $z = 0$. This means we can realize the orthogonal projection onto the affine plane of $g_{f+\varepsilon n} \circ G(i,j)$ by simply ignoring the z-coordinate of vectors. The angles between $\delta_2 f(i,j)$, $\delta_1 f(i,j)$, $\delta_{-2} f(i,j)$ and $\delta_{-1} f(i,j)$ are measured in the plane $z = 0$ and consequently do not change with projection. The angles between the projections of $g_{f+\varepsilon n} \circ G(i,j)$ and the appropriate vectors $\delta_k f(i,j)$ all have the absolute value $\beta := \arctan\frac{\varepsilon\sin\alpha}{l} = \arctan(\varepsilon\omega)$ and their orientation depends on $k \in \{-2,-1,1,2\}$. Figure (20a) shows all those angles as they result from the definitions in section (1.1.4) (see figure (5)). From this follow the angles between the projected generalized Gauss normals — see figure (20b).

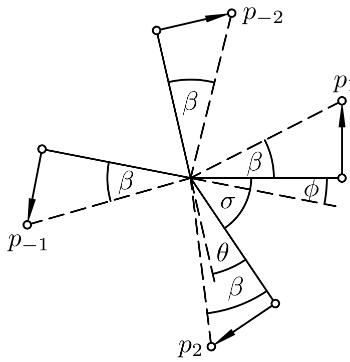

(a) circular net $g_{f+\varepsilon n} \circ G(i,j)$

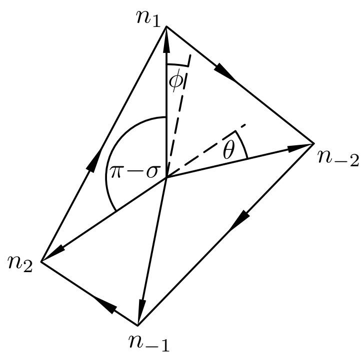

(b) Gauss map $n_g \circ G(i,j)$

Figure 20: circular quadrilaterals

Note that the $n_g \circ G(i,j)$ is traversed clockwise and therefore has negative area. We get

$$A(n_g \circ G) = -\frac{\sin^2\alpha}{8}\big(\sin(\pi - \sigma - \theta + \phi) + \sin(\sigma - \phi) + \sin(\pi - \sigma) + \sin(\sigma + \theta)\big)$$

which can be simplified, using trigonometric formulæ, to

$$A(n_g \circ G) = -\frac{\sin^2\alpha}{2}\sin\left(\sigma - \tfrac{\phi-\theta}{2}\right)\cos\tfrac{\phi}{2}\cos\tfrac{\theta}{2} \tag{63}$$

The circular quadrilaterals $g_{f+\varepsilon n} \circ G$ have the radius $l' := \frac{1}{2}\sqrt{l^2 + \varepsilon^2\sin^2\alpha}$, and their oriented area is

$$A(g_{f+\varepsilon n} \circ G) = \frac{l'^2}{2}\big(\sin(\sigma - \phi + \theta + 2\beta) + \sin(\pi - \sigma + \phi - 2\beta) + \\ + \sin(\sigma + 2\beta) + \sin(\pi - \sigma - \theta - 2\beta)\big)$$

Simplifying this yields

$$A(g_{f+\varepsilon n} \circ G) = 2l'^2 \cos\tfrac{\phi}{2}\cos\tfrac{\theta}{2}\big(\sin 2\beta\cos(\sigma - \tfrac{\phi-\theta}{2}) + \cos 2\beta \sin(\sigma - \tfrac{\phi-\theta}{2})\big)$$

We now use $\sin 2\beta = \sin(2\arctan\varepsilon\omega) = \frac{\varepsilon l \sin\alpha}{2l'^2}$ and $\cos 2\beta = \frac{l^2 - \varepsilon^2\sin^2\alpha}{4l'^2}$ and finally get

$$A(g_{f+\varepsilon n} \circ G) = \tfrac{l^2}{2}\cos\tfrac{\phi}{2}\cos\tfrac{\theta}{2}\big(2\varepsilon\omega\cos(\sigma - \tfrac{\phi-\theta}{2}) + (1-\varepsilon^2\omega^2)\sin(\sigma - \tfrac{\phi-\theta}{2})\big). \tag{64}$$

Steiner's formula describes a relation between the way the area of (smooth) parallel surfaces changes with offset distance and the prinicipal curvatures of the surface. For a twice differentiable surface f for small values of t we can construct smooth parallel surfaces by $f + t\nu$. Steiner's formula is

$$dA(f + t\nu) = (1 - 2Ht + Kt^2)dA(f) \tag{65}$$

where dA is the infinitesimal area form.

In the discrete case we use single faces as infinitesimal area pieces, whose area is given by A. We will be using $g_{f+\varepsilon n} \circ G$ in place of the smooth f at u, and $n_g \circ G$ as ν. So Steiner's formula gives us

$$A(g_{f+(\varepsilon+t)n} \circ G) = (1 - 2Ht + Kt^2)A(g_{f+\varepsilon n} \circ G) \tag{66}$$

and thus

$$\frac{A(g_{f+(\varepsilon+t)n} \circ G)}{A(g_{f+\varepsilon n} \circ G)} = \frac{2(\varepsilon+t)\omega\cos(\sigma - \frac{\phi-\theta}{2}) + (1 - (\varepsilon+t)^2\omega^2)\sin(\sigma - \frac{\phi-\theta}{2})}{2\varepsilon\omega\cos(\sigma - \frac{\phi-\theta}{2}) + (1-\varepsilon^2\omega^2)\sin(\sigma - \frac{\phi-\theta}{2})} = \\ = 1 - 2t\underbrace{\frac{\omega(\varepsilon\omega - \cot(\sigma - \frac{\phi-\theta}{2}))}{1 + 2\varepsilon\omega\cot(\sigma - \frac{\phi-\theta}{2}) - \varepsilon^2\omega^2}}_{=H} + t^2\underbrace{\frac{-\omega^2}{1 + 2\varepsilon\omega\cot(\sigma - \frac{\phi-\theta}{2}) - \varepsilon^2\omega^2}}_{=K}. \tag{67}$$

$$\boxed{K = \frac{-\omega^2}{1 + 2\varepsilon\omega\cot\left(\sigma - \frac{\phi-\theta}{2}\right) - \varepsilon^2\omega^2}} \tag{68}$$

These calculations do not explicitly use n_g at all. We could also calculate K by using $A(n_g \circ G)$ as well, which ultimately results in a simpler formula. A is a quadratic form. We can extend it to a bilinear form the way it is usually done in linear algebra via

$$A(P, Q) := \tfrac{1}{2}\big(A(P+Q) - A(P) - A(Q)\big)$$

which results in

$$\left.\begin{aligned} A(g_{f+(\varepsilon+t)n} \circ G) &= (1-2tH+t^2K)\, A(g_{f+\varepsilon n} \circ G) \\ A(g_{f+(\varepsilon+t)n} \circ G) &= A(g_{f+\varepsilon n} \circ G) + 2tA(g_{f+\varepsilon n} \circ G, n_g \circ G) + t^2 A(n_g \circ G) \end{aligned}\right\}$$

$$\underset{\substack{\uparrow \\ \text{equating coefficients}}}{\Rightarrow} \quad K = \frac{A(n_g \circ G)}{A(g_{f+\varepsilon n} \circ G)}. \tag{69}$$

As mentioned in the beginning of this section the method of derived circular nets can also be used to assign curvatures to the rhombi of the net as opposed to the knots. The calculations are skipped here but the result is:

$$\begin{array}{l}\text{The rhombi } (f, \tau_2 f, \tau_1\tau_2 f, \tau_1 f) \\ \text{have the Gaussian curvature}\end{array} \quad K = \frac{-\omega^2}{\left(\tan\frac{\sigma}{2} + \varepsilon\omega\right)\left(\tan\frac{\overline{\sigma}}{2} - \varepsilon\omega\right)} \tag{70}$$

where $\overline{\sigma}$ is the second internal angle of the rhombi (σ is the first). It can be calculated by $\overline{\sigma} = \pi - \tau_1(\sigma - \phi) = \pi - \tau_2(\sigma - \theta)$ or directly by $\tan\frac{\sigma}{2}\tan\frac{\overline{\sigma}}{2} = \cos\alpha$ which gives

$$\begin{array}{l}\text{The rhombi } (f, \tau_2 f, \tau_1\tau_2 f, \tau_1 f) \\ \text{have the Gaussian curvature}\end{array} \quad K = \frac{-\omega^2}{\cos\alpha + \varepsilon\omega\left(\cos\alpha\cot\frac{\sigma}{2} - \tan\frac{\sigma}{2}\right) - \varepsilon^2\omega^2}. \tag{71}$$

1.4.5 Curvature calculation by net refinement

There also is a way to refine regular and alternating conic nets by constructing a net with halfed edge length such that the original one is an approximation of it. This step can be iterated to form a limiting process, at whose end is a smooth surface whose shape operator is well-defined and whose curvature can be calculated easily.

Other than the previous sections this is not a discrete differential geometric approach, but it serves as an interesting result for comparison. Also it is the approach taken by (W. Wunderlich 1952).

As we construct a sequence of conic nets with $l \to 0$ it is obviously neccessary to have $\alpha \to 0$ as well. We realize this by demanding $\omega = \text{const}$.

Formally we replace f by

$$f_l \colon (l\mathbb{Z})^2 \to \mathbb{R}^3. \tag{72}$$

We know, that, apart from l, α and $\sigma(0,0)$ (which will stay constant as well), the shape of f is governed by the two functions $\phi(.,0)$ and $\theta(0,.)$. How can we refine those?

One simple way is to take two Lipschitz continuous functions $\phi \colon \mathbb{R} \to \mathbb{R}$ and $\theta \colon \mathbb{R} \to \mathbb{R}$ and define

$$\begin{aligned} &\phi_l(.,0) \colon l\mathbb{Z} \to \mathbb{R},\ i \mapsto \phi((i+1)l) - \phi(il) \quad \text{and} \\ &\theta_l(0,.) \colon l\mathbb{Z} \to \mathbb{R},\ j \mapsto \theta((j+1)l) - \theta(jl) \end{aligned} \tag{73}$$

which keeps

$$\phi_l(i,0) = \sum_{i'=0}^{2^m-1} \phi_{2^{-m}l}(i + i'2^{-m}l, 0)$$

so refined nets will approximate the shapes of previous ones and at the same time ensures $\lim_{l\to 0}\sup_{i\in l\mathbb{Z}}|\phi_l(i,0)| = 0$ and likewise for θ.

Now we use the calculations from section (1.4.2) with f_l instead of f and obtain

$$\nabla\nu\big|_0 \approx \left(\frac{\delta_1 n_l}{l}, \frac{\delta_2 n_l}{l}\right)(0,0) = \left(\left(\begin{smallmatrix}0\\ \omega\\ \omega\tan\frac{\alpha_l}{2}\end{smallmatrix}\right), \mathrm{rot}^{e_3}_{-\sigma(0,0)}\left(\begin{smallmatrix}0\\ -\omega\\ \omega\tan\frac{\alpha_l}{2}\end{smallmatrix}\right)\right)$$

and

$$\nabla f\big|_0 \approx \left(\frac{\delta_1 f_l}{l}, \frac{\delta_2 f_l}{l}\right)(0,0) = \left(\left(\begin{smallmatrix}1\\ 0\\ 0\end{smallmatrix}\right), \mathrm{rot}^{e_3}_{-\sigma(0,0)}\left(\begin{smallmatrix}1\\ 0\\ 0\end{smallmatrix}\right)\right).$$

Now we take the limits of those observing $\omega = \text{const.}$ and obtain

$$\nabla\nu\big|_0 = \lim_{l\to 0}\left(\frac{\delta_1 n_l}{l}, \frac{\delta_2 n_l}{l}\right)(0,0) = \left(\left(\begin{smallmatrix}0\\ \omega\\ 0\end{smallmatrix}\right), \mathrm{rot}^{e_3}_{-\sigma(0,0)}\left(\begin{smallmatrix}0\\ -\omega\\ 0\end{smallmatrix}\right)\right) \tag{74}$$

$$\nabla f\big|_0 = \lim_{l\to 0}\left(\frac{\delta_1 f_l}{l}, \frac{\delta_2 f_l}{l}\right)(0,0) = \left(\left(\begin{smallmatrix}1\\ 0\\ 0\end{smallmatrix}\right), \mathrm{rot}^{e_3}_{-\sigma(0,0)}\left(\begin{smallmatrix}1\\ 0\\ 0\end{smallmatrix}\right)\right). \tag{75}$$

Which is the same result as when forcing the derivatives of n into the knot plane in section (1.4.2). We therefore get the same Gaussian curvatures.

1.4.6 Comparison of results

The results for Gaussian curvatures we calculated in the last sections are

knots	Central differences; derived circular nets	$\dfrac{-\omega^2}{1+2\varepsilon\omega\cot\left(\sigma-\frac{\phi-\theta}{2}\right)-\varepsilon^2\omega^2}$
knots	Forced one-sided differences; limiting process	$\dfrac{-\omega^2}{1+2\varepsilon\omega\cot\sigma-\varepsilon^2\omega^2}$
rhombi	Derived circular nets	$\dfrac{-\omega^2}{\cos\alpha+\varepsilon\omega\left(\cos\alpha\cot\frac{\sigma}{2}-\tan\frac{\sigma}{2}\right)-\varepsilon^2\omega^2}$

If we replace α, θ and ϕ by α_l, θ_l and ϕ_l and calculate the limits $l\to 0$ we see that all version of the Gaussian curvature converge to the version found via net refinement (the rhombus curvature too, as $\cot\frac{\sigma}{2}-\tan\frac{\sigma}{2} = 2\cot\sigma$).

In the case $\varepsilon = 0$ (rhombic nets with planar knots) we find in every case $K = -\omega^2$ for knots and $K = -\omega^2/\cos\alpha$ for rhombi, which means, as expected, constant negative Gaussian curvature.

There is another thing worth noting: (W. Wunderlich 1952) studied the circles through pairs of opposite knots of a rhombus of a rhombic net with planar knots, whose centers M and M' are the intersection points of the appropriate knot normals. See figure (21).

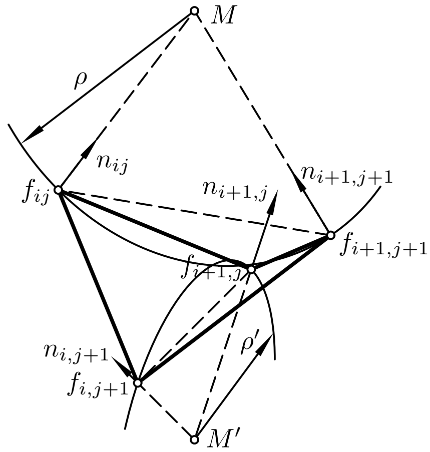

Figure 21: circles through opposite knots

Wunderlich calculated the product $\rho\rho'$ and found it to be constant for all rhombi of a net. Interestingly it is just the reciprocal of the curvature of the rhombus as defined by using derived circular nets.

$$-\rho\rho' = -\frac{\cos\alpha}{\omega^2} = K^{-1} \tag{76}$$

This suggests considering these circles for conic nets. We see that when we apply an offset to the rhombic net with planar knots the radii change to $\rho \mapsto \rho - \varepsilon$ and $\rho' \mapsto \rho' + \varepsilon$, respectively. We find that in this case the product matches the calculated rhombus curvature too, which gives us a nice way of understanding rhombus curvatures geometrically:

$$-(\rho\rho')^{-1} = \frac{-\omega^2}{\cos\alpha + \varepsilon\omega\big(\cos\alpha\cot\frac{\sigma}{2} - \tan\frac{\sigma}{2}\big) - \varepsilon^2\omega^2} = K. \tag{77}$$

2 Rhombic nets optimization

2.1 General things

2.1.1 Additional definitions

In addition to the definitions set forth in section (1.1.1) we will fix a couple of other notations which will be used frequently.

- $\mathcal{P}(p,q) \subseteq R^3$, $p,q \in \mathbb{R}^3$, $q \neq 0$ is the plane which contains q and has the normal p, that is
$$\mathcal{P}(p,q) = \{s \in \mathbb{R}^3 \colon \langle s-q, p\rangle = 0\}.$$
- $\pi_A \colon \mathbb{R}^3 \to A$ is the orthogonal projection operator onto the plane A. In particular we will be using
$$\pi_{\mathcal{P}(e_3,0)} = \text{ projection onto the plane } z=0. \tag{78}$$
- The unit sphere $S_1 := \{p \in \mathbb{R}^2 \colon \|p\| = 1\}$.

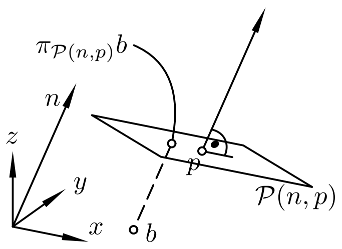

Figure 22: Planes and orthogonal projections

In addition to rhombic nets we will be dealing with general triangle meshes. $\mathcal{M}$ will in the following always denote such a mesh. It consists of sets of *vertices*, $\mathcal{V} \subset \mathbb{R}^3$, *combinatorical edges* $\mathcal{E}_c \subset \mathcal{V}^2$, that is pairs of vertices connected by an edge and, likewise, *combinatorical faces* $\mathcal{F}_c \subset \mathcal{V}^3$.

These result in *edges*

$$\mathcal{E}(p,p') := \{p(1-t) + p't \colon t \in [0,1]\}, \text{ where } (p,p') \in \mathcal{E}_c \tag{79}$$

and *faces*

$$\mathcal{F}(p,p',p'') := \{pt + p't' + p''t'' \colon t,t',t'' \in [0,1] \text{ with } t+t'+t'' = 1\}. \tag{80}$$

We will always assume that all faces are nondegenerated, that is, their 3 corners are affinely independent. We will further assume that $\mathcal{M}$ has the following properties:

- The orthogonal projection of $\mathcal{M}$ onto the plane $z=0$, $\pi_{\mathcal{P}(e_3,0)}\big|_{\mathcal{M}}$, is injective. In particular there is an eulerian parametrization of $\mathcal{M}$ in the form
$$(x,y)^T \mapsto \big(x,y,f(x,y)\big)^T.$$
Let (p,p',p'') be a combinatorical face of $\mathcal{M}$, then for a normal of that face $(p'-p)\times(p''-p)$ follows $z\big((p'-p)\times(p''-p)\big) \neq 0$.
- $\pi_{\mathcal{P}(e_3,0)}(\mathcal{M})$ is a convex set.

2.1.2 Halfedge data structures

The following sections all deal with algorithms on triangle meshes that are meant to be implemented on computers. Therefore we will have to confine ourselves to finite meshes.

There are various methods of storing meshes in computer memory. The easiest one is to store vertices, combinatorical faces and, if necessary, combinatorical edges in seperate vectors. In this it is reasonable to store combinatorical faces and edges as pairs and triples of *indices* into the vertex vector.

A simple data structure like that has serious downsides. The algorithms in this thesis will for example need to traverse meshes by moving from a face to an adjacent face a lot. With the mentioned data structure this is a fast operation only if there are additional assumptions about the mesh, e.g. that its structure is in some way regular. Without getting formal, figure (23) makes it clear what might constitute a regular structure.

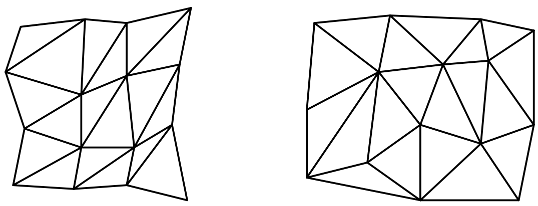

(a) Regular mesh (b) Irregular mesh

Figure 23: Regular and irregular triangle meshes

In practive there are indeed situations where we have to deal with irregular meshes, in particular meshes that result from 3D scanning and subsequent optimization. In these cases finding adjacent faces takes linear time. We can solve this problem by using a more complex data structure to store meshes.

From several possibilities the well-known *halfedge* data structure was chosen. It was introduced by (K. Weiler 1985). There is a comprehensive description of it in (M. Mäntylä 1988), for example.

A halfedge may be thought of as an arrow along a mesh edge that points from one vertex towards the other (oriented edge). Halfedges are associated with a face of the mesh of which they describe a adge. Therefore for internal edges of the mesh there are two halfedges, respectivey. (We will always exclude meshes where there are edges adjacent to more than two faces.) Each one is called the counter edge to the other. Additionally each halfedge stores information on which halfedges are the next (and, optionally, the previous one as well) along the face's border. Obviously this approach is not limited to triangular faces, but we will still limit ourselves to triagular meshes for reasons of simplicity, because triangular faces can be seen as (planar) surfaces in an obvious way (and therefore have a unique normal). Halfedges store a reference to one of their vertices too — it is not determined which one, but we will always store the *first* vertex of every halfedge.

For algorithms using a halfedge structure being able to work properly it is often necessary to assume that pairs of counter edges are oriented reciprocally. This is not possible for all meshes. It turns out that the meshes that allow a halfedge structure are the discrete analoga of those differentiable surfaces that have a continuous gauss map (orientable surfaces). Figure (24) shows an example of a mesh that does not have this property.

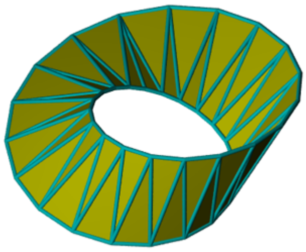

Figure 24: Discrete Möbius strip

This might be considered a shortcoming of the halfedge approach but also a strength as many algorithms assume surfaces to be orientable and this way it can be easily checked if given meshes satisfy the condition.

We will be using the nomenclature shown in figure (25), which uses the arrow symbol (→), borrowed from the C and C++ programming languages to pass from a halfedges to one of its references (previous, next and counter halfedges, adjacent face, first vertex).

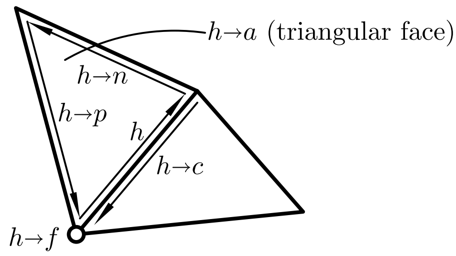

Figure 25: References stored by a halfedge h — Nomenclature

Additionally each face a stores a reference $a{\to}f$ to one of its halfedges (any one).

There are two possibilities for assigning halfedges to a face: clockwise and counter-clockwise. Once one of these orientations is chosen, those of adjacent faces follow uniquely. A problem can occur if the mesh comprises several unconnected parts. We exclude this cases with the following theorem:

Theorem 2.1. *A mesh $\mathcal{M}$ that satisfies the properties stated in section (2.1.1) is simply connected and does allow a halfedge structure, where the chosing of the orientation of a single face determins the orientation of all other faces.*

Proof. Omitted. □

From this we can simply calculate face normals. If $h := a{\to}f$ is a halfedge of the face a we define the normal

$$a{\to}n := \frac{(h{\to}n{\to}f - h{\to}f) \times (h{\to}p{\to}f - h{\to}f)}{\left\|(h{\to}n{\to}f - h{\to}f) \times (h{\to}p{\to}f - h{\to}f)\right\|} \tag{81}$$

2.2 Statement of the problem and overview

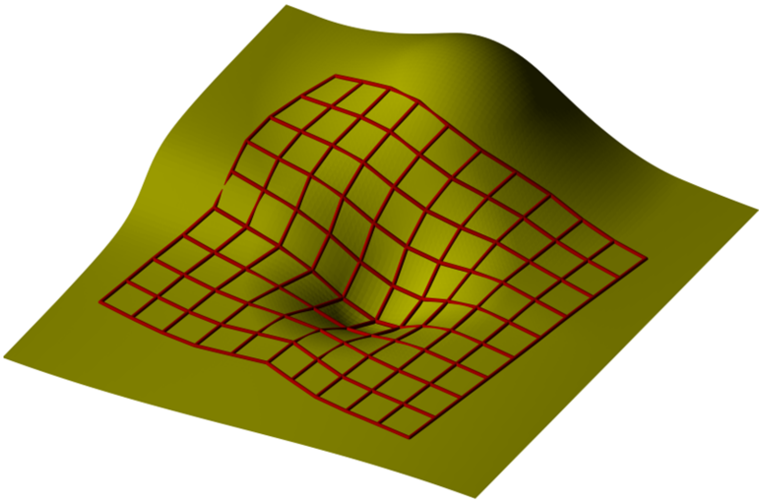

The aim of this section is, for a given mesh $\mathcal{M}$ which has the properties from section (2.1.1) and $r > 0$, to find a finite net f_{ij}, $i = 1, \dots, n$, $j = 1, \dots, m$ that overlays $\mathcal{M}$ with a rhombic net, that is

- $\|f_{ij} - f_{i-1,j}\| = r$, $(i, j) \in \{2, \dots, n\} \times \{1, \dots, m\}$ and $\|f_{ij} - f_{i,j-1}\| = r$, $(i, j) \in \{1, \dots, n\} \times \{2, \dots, m\}$.
- $p_{i,j} \in \mathcal{M}$, $(i, j) \in \{1, \dots, n\} \times \{1, \dots, m\}$ (The knots of p all lie on the mesh surface.)
- The rhombic net will be optimal in a sense yet to be defined.

Rhombic nets on a surface have a lot of degrees of freedom. In our case (n lines, m columns) we get $m + n$ degrees of freedom.

We will reduce this number by freely chosing the first knot $\in \mathcal{M}$ and laying out the first row of knots straight in a direction that can also be freely chosen. After that the remaining knots are calculated linewise such that every successive line is optimal.

On the while the procedure is the following:

1. Fix the starting point p_{11}. It has to lie on one of the triangular faces. Call that face f.

2. Construct the first row of rhombus knots. A knot p_{1i} is formed by moving from $P_{1,i-1}$ along a curve that is the intersection of the surface $\mathcal{M}$ and a plane through $p_{1,i-1}$ with normal vector ε_i, until we reach a point such that $\|p_{1i} - p_{1,i-1}\| = 5$. See figure (26). The vectors ε_i can be chosen freely with certain constraints. We will usually use $y(\varepsilon_i) = 0$. If we want to lay out the first row of knots "straight" this means $\varepsilon_i = \varepsilon_1$, $i = 1, \dots, m$.

3. We form a closed curve L_i that is the intersection of $\mathcal{M}$ and the sphere with radius r around p_{1i}. Obviously $p_{2i} \in L_i$ has to hold $\forall\, i$. L_i consists of pieces of circles with centers in p_{1i}.

In addition we fix a family of functions $\Psi_i \colon L_i \to [0,1]$ which evaluate the possible choices of p_{2i}, where $\Psi_i(p_{2i}) = 0$ is optimal.

If $p_{21}, \dots, p_{2m}$ is a well-formed second row (that is, $\|p_{2i} - p_{2,i-1}\| = r \; \forall\, i \in \{2, \dots, m\}$), we evaluate the complete row by

$$\Psi(p_{21}, \dots, p_{2m}) := \max\bigl\{\Psi_1(p_{21}), \dots, \Psi_m(p_{2m})\bigr\}. \tag{82}$$

4. We want to find that row $p_{21}, \dots, p_{2m}$ such that $\Psi(p_{21}, \dots, p_{2m})$ is minimal.

   For this we fix a continuous parametrization of L_1 and thus obtain a function $p_{21}(t)$. For every t the values of p_{2i}, $i = 2, \dots, m$ can be calculated successively by means of the condition $\|p_{2i} - p_{2,i-1}\| = r$. In this way we realize a functions $t \mapsto \Psi\bigl(p_{21}(t), \dots, p_{2m}(t)\bigr)$. To this we apply the *golden section search* algorithm to numerically find the minimum.

5. Steps 3 and 4 are iterated to construct arbitrarily many rows of knots.

In the following these steps are described in detail.

2.2.1 Step 1

In this step we have a point $p \in \mathbb{R}^3$ and wish to find a point $p' \in \mathcal{M}$ with $p - p' \propto e_3$ and a combinatorical face $(a, b, c) \in \mathcal{F}_c$ such that p' lies in that face $\mathcal{F}(a, b, c)$, which means projecting p onto the mesh along e_3.

This problem needs to be solved only once in the whole optimization procedure, therefore a brute-force approach will be sufficient.

The assumption that $\pi_{\mathcal{P}(e_3,0)}\big|_{\mathcal{M}}$ is injective enables us to search for p' in that plane:

$$p' \in \mathcal{F}(a, b, c) \Leftrightarrow \pi_{\mathcal{P}(e_3,0)} p \in \mathcal{F}(\pi_{\mathcal{P}(e_3,0)} a, \pi_{\mathcal{P}(e_3,0)} b, \pi_{\mathcal{P}(e_3,0)} c) \subset \mathbb{R}^2 \times \{0\} \tag{83}$$

Therefore we can simply ignore the z component of all occuring points.

If a triangle $(a, b, c) \subset \mathbb{R}^2$ is oriented in such a way that the edges (a, b), (b, c), (c, a) traverse the border in the positive direction a point $q \in \mathbb{R}^2$ lies inside the triangle (or on its border) if and only if it lies at the left of all the edges, that is

$$\det(b - a, q - a),\ \det(c - b, q - b),\ \det(a - c, q - c) \geq 0. \tag{84}$$

The calculation of these two-dimensional determinants is a fairly fast operation but it is unnecessary in most cases: a point can only lie in a triangle (a, b, c) if it lies in the triangle's boundary rectangle $\bigl[\min\{x(a), x(b), x(c)\}, \max\{x(a), x(b), x(c)\}\bigr] \times \bigl[\min\{y(a), y(b), y(c)\}, \max\{y(a), y(b), y(c)\}\bigr]$.

After the combinatorical face is found the point p' (in $\mathbb{R}^3$) is simply found by intersecting $p + e_3\mathbb{R}$ with the face's plane.

Below is the whole procedure as a pseudocode algorithm:

Algorithm 2.1. (Solution of step 1)

```
Input: p ∈ ℝ³
for f ∈ F_c do
    h := f→f, a₁ := h→f, a₂ := h→n→f, a₃ := h→p→f
```

4: $[x_{\min}, x_{\max}] := [\min_{i=1,2,3} x(a_i), \max_{i=1,2,3} x(a_i)]$ and
$[y_{\min}, y_{\max}] := [\min_{i=1,2,3} y(a_i), \max_{i=1,2,3} y(a_i)]$.
5: **if** $x(p) \in [x_{\min}, x_{\max}] \wedge y(p) \in [y_{\min}, y_{\max}]$ **then**
6: **if** $\det_{2\mathrm{D}}(a_2 - a_1, q - a_1) \geq 0 \wedge \det_{2\mathrm{D}}(a_3 - a_2, q - a_2) \geq 0 \wedge$
$\det_{2\mathrm{D}}(a_1 - a_3, q - a_3) \geq 0$ **then**
7: (f is the resulting combinatorical face.)
8: **return** $p' := p + e_3 \frac{\langle a_1 - p, f \to n\rangle}{z(f \to n)}$
9: **end if**
10: **end if**
11: **end for**
12: **return** *false*

Here $\det_{2\mathrm{D}} \colon \mathbb{R}^3 \times \mathbb{R}^3 \to \mathbb{R}, (a, b) \mapsto x(a)y(b) - y(a)x(b)$ denotes the determinant in the plane $z = 0$.

The general assumption of $\pi_{\mathcal{P}(e_3,0)}\big|_{\mathcal{M}}$ being injective guarantees that for all face normals n of faces of $\mathcal{M}$ there is $z(n) \neq 0$. Therefore p' is well-defined by line (8) of the algorithm.

Note that the result of this step is not unique if p' lies in an edge of the mesh. In that case the result depends on the order in which the combinatorical faces are stored in $\mathcal{F}_c$.

The algorithm fails if and only if $\pi_{\mathcal{P}(e_3,0)} p \notin \pi_{\mathcal{P}(e_3,0)}(M)$.

If the triangles of $\mathcal{M}$ are very small it might be considered to skip this step altogether and simply chose some vertex of $\mathcal{M}$ as p'.

2.2.2 Step 2

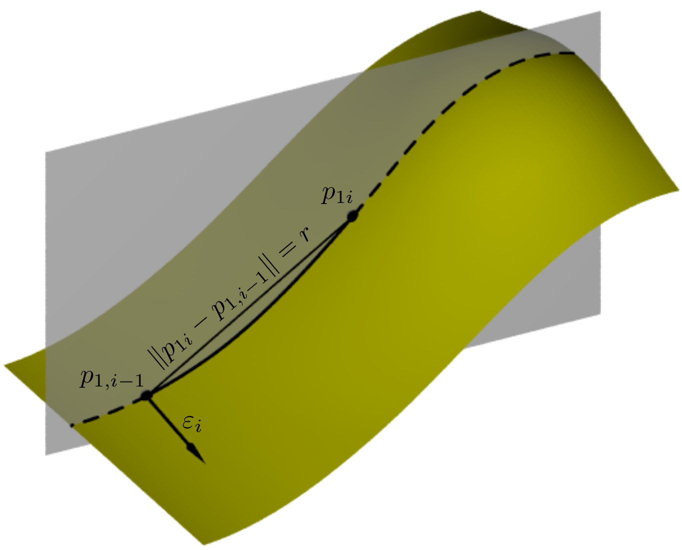

Figure 26: Task of step 2

In this step we want to find, for a point $p \in \mathcal{M}$, another point $p' \in \mathcal{M}$ with $\|p - p'\| = r$ such that, in simple terms, p' seen from p lies in a certain direction.

We will exploit that $\mathcal{M}$ can be projected orthogonally onto the $z = 0$ plane (assumption 1 in section (2.1.1)) by demanding that

$$\pi_{\mathcal{P}(e_3,0)}(p') = \pi_{\mathcal{P}(e_3,0)}(p) + \lambda \frac{v}{\|v\|} \text{ for some } \lambda > 0,$$

that is that p', *when viewed from above* lies in the direction v from p. This is equivalent to p' lying in the plane spanned by v and e_3. We define this plane in terms of its unity normal vector

$$\varepsilon = \frac{v \times e_3}{\|v \times e_3\|} = \left(x(v)^2 + y(v)^2\right)^{-\frac{1}{2}} \left(\begin{smallmatrix} y(v) \\ -x(v) \\ 0 \end{smallmatrix}\right). \tag{85}$$

The condition $\langle p' - p, \varepsilon\rangle = 0$ together with $p' \in \mathcal{M}$ and $\|p' - p\| = r$ most of the time has solutions $\pi_{\mathcal{P}(e_3,0)}(p') = \pi_{\mathcal{P}(e_3,0)}(p) + \lambda v/\|v\|$ with both $\lambda > 0$ and $\lambda < 0$. We are only interested in those with $\lambda > 0$. Thus we add another condition to exclude the other solution. As we want to work throughout with ε we put it in the form $\det(\varepsilon, p' - p, e_3) > 0$.

Putting everything together results in the following problem:

Problem 2:

Let $p \in \mathcal{M}$ and $\varepsilon \in S_1$ with $z(\varepsilon) = 0$. The task is to find a point $p' \in \mathcal{M}$, which satisfies the following conditions:

(a) $\langle p' - p, \varepsilon\rangle = 0$,

(b) $\|p' - p\| = r$,

(c) $\det\left(\varepsilon, p' - p, e_3\right) > 0$.

Is the solution of this problems (if one exists) unique under the stated conditions? At least we see

Theorem 2.2. *If there is a solution to problem 2, then it is unique, provided that* $z(f \to n) \geq 2^{-1/2}\ \forall f \in \mathcal{F}_c$.

Proof. Assume that there are two different solutions, p' and p''. Consider the intersection plane $\mathcal{P}(\varepsilon, p)$: The points of the circle around p in this plane with radius r are obviously exactly those that satisfy conditions (2.a) and (2.b). $\mathcal{M} \cap \mathcal{P}(\varepsilon, p)$ is a curve through p that can be injectively orthogonally projected onto a horizontal line. As $p', p'' \in \mathcal{M}$ both p' and p'' lie on this curve. Because of (2.c) they lie on the same side of p. Figure (27) illustrates this situation.

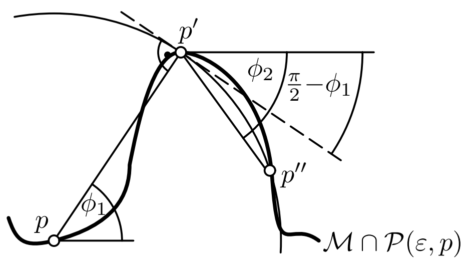

Figure 27: Multiple solutions of problem 2

Obviously there must be $\phi_2 > \frac{\pi}{2} - \phi_1$. From this follows that the maximum absolute value of the incline of the curve must be at least

$$\max\{\phi_1, \phi_2\} = \max\{\phi_1, \frac{\pi}{2} - \phi_1 + \alpha\} =: c \text{ for some } \alpha > 0.$$

This term attains its minimum if $\phi_1 = \phi_2 \Rightarrow \phi_1 = \frac{\pi}{4} + \frac{\alpha}{2}$ and therefore (as $\alpha > 0$) we find $c > \frac{\pi}{4}$.

If we assume that the normals of the faces of $\mathcal{M}$ deviate from e_3 by angles at most $\frac{\pi}{4}$ (from which follows that the absolute value of the incline of surface curves can not be larger either) this situation is excluded.

$$\arccos\langle f{\to}n, e_3\rangle \leq \frac{\pi}{4} \quad \Leftrightarrow \quad z(f{\to}n) \geq \frac{1}{\sqrt{2}} \; \forall\, f \in \mathcal{F}_c. \qquad \square$$

It would not be a severe problem to limit ourselves to meshes $\mathcal{M}$ with this additional property but it turns out that this is not neccessary.

The following algorithm finds a solution of problem 2 by traversing the curve $\mathcal{M} \cap \mathcal{P}(\varepsilon, p)$ starting at p until the circle is reached. Therefore the solution will always be that which is denoted p' in figure (27). That there may be different solutions beyond it is not a problem.

Algorithm 2.2. (Solution of step 2)

Input:
- (i) $f \in \mathcal{F}_c$
- (ii) $p \in \mathcal{F}(f)$ (p is a point of the surface of f.)
- (iii) $\varepsilon \in S_1$ with $z(\varepsilon) = 0$.

$h := f{\to}f,\; t_p := \langle p, \varepsilon\rangle,\; t_0 := \langle f{\to}f, \varepsilon\rangle$ and $p_0 := p$.

loop
- $t_1 := t_0,\; t_0 := \langle h{\to}n{\to}f, \varepsilon\rangle$
- **if** $t_p \in [t_0, t_1]$ **then**
  - $p_1 := p_0$
  - $$p_0 := \begin{cases} \dfrac{(t_p - t_0)\cdot h{\to}f + (t_1 - t_p)\cdot h{\to}n{\to}f}{t_1 - t_0}, & \text{if } t_0 \neq t_1 \\ h{\to}f, & \text{if } t_0 = t_1 \text{ and } \det\big(\varepsilon, h{\to}f - h{\to}n{\to}f, e_3\big) > 0 \\ h{\to}n{\to}f, & \text{else} \end{cases}$$
  - **if** $\|p_0 - p\| \geq r$ **then** // $\Rightarrow p'$ must lie between p_0 and p_1.
    - $p' := t\,p_0 + (1-t)\,p_1$, where t results from the quadratic equation $\|t\,p_0 + (1-t)\,p_1 - p\| = r$.
    - **return** *true* // success
  - **end if**
  - $t_0 := t_1$
  - **if** $\nexists\, h{\to}c$ **then** **return** *false* // reached the border of $\mathcal{M} \Rightarrow$ algorithm failed
  - **else** $h := h{\to}c{\to}n$
  - **end if**
- **else** $h := h{\to}n$
- **end if**

end loop

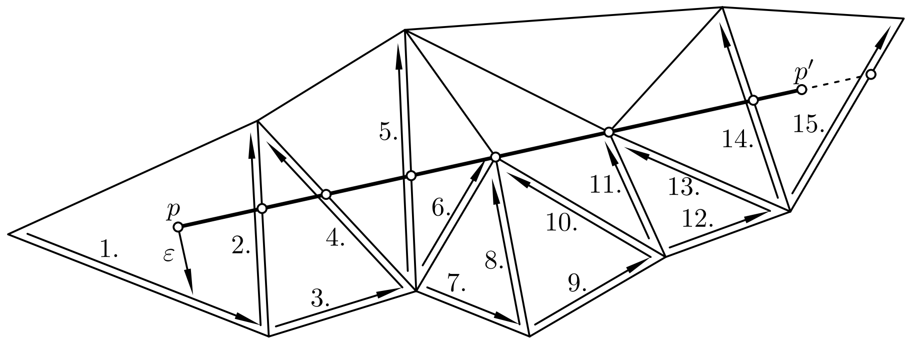

Figure 28: Algorithm (2.2) example

Figure (28) illustrates the order in which halfedges are traversed.

The algorithm can terminate in two different ways.

return true means that a p' was found that solves problem 2.

return false occurs when the intersection curve $\mathcal{M} \cap \mathcal{P}(\varepsilon, p)$ reaches the border of $\mathcal{M}$ before a solution is found. If a solution of problem 2 existed this would contradict the assumption that the orthogonal projection of $\mathcal{M}$ onto the $z = 0$ plane $\pi_{\mathcal{P}(e_3,0)}(\mathcal{M})$ is convex (see section (2.1.1)). Therefore there is no solution.

Obviously we could exclude this case by chosing p such that the distance of $\pi_{\mathcal{P}(e_3,0)}(p)$ to $\pi_{\mathcal{P}(e_3,0)}(\mathcal{M})$ is more than r. We will be using the same assumption in step 3.

2.2.3 Step 3

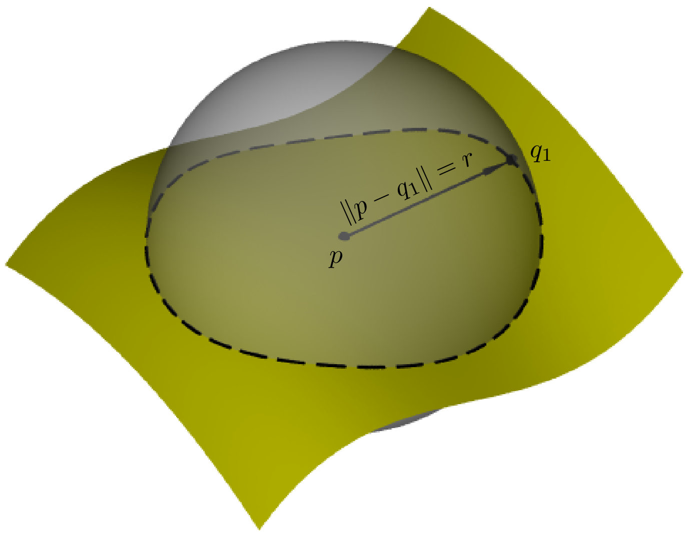

Figure 29: Task of step 3

In this step we basically want to find, for a point $p \in \mathcal{M}$ and $r > 0$, a curve that is the intersection of $\mathcal{M}$ and the sphere with radius r around p.

The intersection of a plane and a sphere is a circle and therefore, as $\mathcal{M}$ consists of triangle faces, this curve consists of pieces of circles that lie in the respective faces, with the start and end points on the border of the faces. Intersecting a plane with a sphere is an easy operation so the essential task is to find these start and end points and the edges they lie on.

We start at p itself and employ algorithm (2.2) to reach a point $q_0 \in \mathcal{M}$ with $\|p - q_0\| = r$. After that we wollowe the desired curve by passing from one face f through that edge of f where the curve exits f to the face adjacent to f at this edge.

Theorem 2.3. *The solution of problem 3 is unique, provided that $z(f{\to}n) \geq 2^{-1/2}\ \forall f \in \mathcal{F}_c$.*

Proof. Assume the solution is not unique. That means that there are two injective paths f_1 and f_2 such that $f_i(0) = f_i(1) = p_0$, $i = 1,2$ but $f_1([0,1]) \neq f_2([0,1])$. Therefore there is some maximal $t \in [0,1)$ such that $f_2([0,t]) \subset f_1([0,1])$ and some $\varepsilon > 0$ such that $f_2((t, t+\varepsilon]) \cap f_1([0,1]) = \emptyset$. This means we have three injective paths $g_1 := s \mapsto f_2(s\varepsilon + t)$, $g_2 := s \mapsto f_2(t(1-s))$ and $g_3 := f_1((1-t')s + t')$ for that t' with $f_1(t') = f_2(t)$ with

$$g_i(0) = p_0 \quad \text{and} \quad g_i([0,1]) \cap g_j([0,1]) = \{p_0\} \quad i,j \in \{1,2,3\},\ i \neq j.$$

New consider these paths in cylindrical coordinates with the cylinder axis

Now we discern two cases:

- $\exists\, i,j,\ i \neq j\colon \phi(g_i(1)) = \phi(g_i(1))$. Then the plane $P\Big(\Big(\begin{smallmatrix} \sin\phi(g_i(1)) \\ -\cos\phi(g_i(1)) \\ 0 \end{smallmatrix}\Big), 0\Big)$ intersects $\mathcal{M} \cap S_1$ in two different places.
- $\nexists\, i,j,\ i \neq j\colon \phi(g_i(1)) = \phi(g_i(1))$. Assume w.l.o.g. $\phi(g_1(1)) < \phi(g_2(1)) < \phi(g_3(1))$. So if we combine g_1 and g_2 into a single path

  $$g(s) := \begin{cases} g_1(1-2s), & s \leq 1/2 \\ g_3(2s-1), & s > 1/2 \end{cases}$$

  due to the intermediate value theorem there is some $s \in [0,1]$ such that $\phi(g(s)) = \phi(g_2(1))$. So we can use the plane $P\Big(\Big(\begin{smallmatrix} \sin\phi(g_2(1)) \\ -\cos\phi(g_2(1)) \\ 0 \end{smallmatrix}\Big), 0\Big)$.

In both cases we get a plane in which *problem 2* of the previous section has two solutions. Theorem (2.2) allows us to exclude this possibility by assuming $z(f{\to}n) \geq 2^{-1/2}\ \forall f \in \mathcal{F}_c$. $\square$

Unlike as in the previous section we cannot ignore the assumption $z(f{\to}n) \geq 2^{-1/2}\ \forall f \in \mathcal{F}_c$ in the algorithm below, so we have to assume that property for the mesh $\mathcal{M}$.

But the assumption is very constrictive, as it is not uncommon for practical surfaces to violate it. It is however possible to replace the assumption with one that is usually satisfied.

Theorem (2.2) and theorem (2.3) also use the assumed property locally, that is for mesh faces that at least partially lie inside the closed sphere with radius r around p. The property of problem 2 and 3 having unique solutions is invariant under rotations of $\mathcal{M}$ around p. Therefore the existence of a unit vector v such that $\langle v, f{\to}n\rangle \geq 2^{-1/2}$ for these faces is sufficient.

We transform this with the Cauchy-Schwarz inequality. Let n, n' be two unit face normals of faces in ...

$$\left.\begin{array}{l}\langle v,n\rangle \geq 2^{-1/2}\\ \langle v,n'\rangle \geq 2^{-1/2}\end{array}\right\} \Rightarrow 2 \leq \langle v, n+n'\rangle^2 \leq \underset{\substack{\uparrow\\ =1}}{\|v\|^2}\, \|n+n'\|^2 = \|n\|^2 + 2\langle n,n'\rangle + \|n'\|^2 \tag{86}$$

which, as $\|n\| = \|n'\| = 1$ results in $\langle n,n'\rangle > 0$. But unfortunately the converse does not hold, as the example $N = \{e_1, e_2, e_3\}$ shows. But we can use a somewhat stronger assumption.

Lemma 3. *Let $N \subset S_1$ such that $\forall\, n, n' \in N$ there is $\langle n, n'\rangle \geq \frac{1}{2}$. Then there exists a $v \in S_1$ such that*

$$\langle v, n\rangle \geq \frac{1}{\sqrt{2}}\ \forall\, n \in N$$

Proof. Let $p \in N$, then $N \subseteq \{q \in S_1\colon \langle q,p\rangle \geq \frac{1}{2}\}$. Assume w.l.o.g. $p = e_1$. Then all points q in N have, when described in cylindrical coordinates $q = r\operatorname{rot}_{\phi}^{e_3} e_1 + ze_3$, angles $\phi \in [-\frac{\pi}{3}, \frac{\pi}{3}]$. Rotate N by the minimal positive angle ϕ_0 such that the cylindrical angles of $q \in N$ are all $\phi \in [-\frac{\pi}{6}, \frac{\pi}{2}]$. Then $y(q) \geq \sin\big(-\frac{\pi}{6}\big) = -\frac{1}{2}$ and there exists a $q_0 \in \overline{N}$ for which there is equality. By the lemma's assumption $\langle q, q_0\rangle \geq \frac{1}{2}$ we see $\|q - q_0\| \underset{\substack{\uparrow\\ q,q_0\in S_1}}{=} 2 - 2\langle q, q_0\rangle \leq 1$ and therefore

$$y(q) \in \big[-\tfrac{1}{2}, \tfrac{1}{2}\big]\ \forall\, q \in N. \tag{87}$$

We now repeat the same argument respective to the z axis. The occuring rotation is around the y axis and therefore does not change the validity of equation (87). We additionally see

$$y(q), z(q) \in \big[-\tfrac{1}{2}, \tfrac{1}{2}\big] \text{ and } x(q) \geq 0\ \forall\, q \in N.$$

From $q \in N \subset S_1$ we see $x(q) = \big(1 - y(q)^2 - z(q)^2\big)^{1/2} \geq \frac{1}{\sqrt{2}}$. Now we simply let $v := e_1$ and get the desired inference. $\square$

This now enables us to state a sufficient condition for the uniqueness of the solution in an easy way. If the mesh $\mathcal{M}$ satisfies the following condition:

> For every $p \in \mathcal{M}$ and every pair of faces f and f' with $f \cap B_r(p), f \cap B_r(p) \neq \emptyset$ for the faces' normals holds
>
> $$\langle n, n'\rangle \geq \tfrac{1}{2}. \tag{88}$$

then solutions to problem 3 are unique.

We can now give an algorithm that solves problem 3.

Algorithm 2.3. (Solution of step 3)

$h_0 := h$
repeat
    $A := h{\to}n{\to}f - h{\to}f, \quad B := h{\to}n{\to}f - M, \quad \gamma := \|B\|^2 - r^2$

```
4:      if γ = 0 ∧ ⟨A, B⟩ ≤ 0 then
5:          There is a new point, namely (h→n→f, h).
6:          repeat
7:              if ∄ h→c then  return false  end if        // reached border
8:              h := h→c→p
9:          until ⟨h→n→f − h→f, h→n→f − M⟩ > 0
10:         h := h→p
11:         goto (20)
12:     end if
13:     α := ‖A‖², β := ⟨A, B⟩, Δ := β² − αγ
14:     if Δ > 0 und t := (β+√Δ)/α ∈ (0, 1) then
15:         There is a new point, namely (h→n→f − tA, h).
16:         if ∄ h→c then  return false  end if        // reached border
17:         h := h→c→n
18:     else h := h→n
19:     end if
20: until h = h₀
```

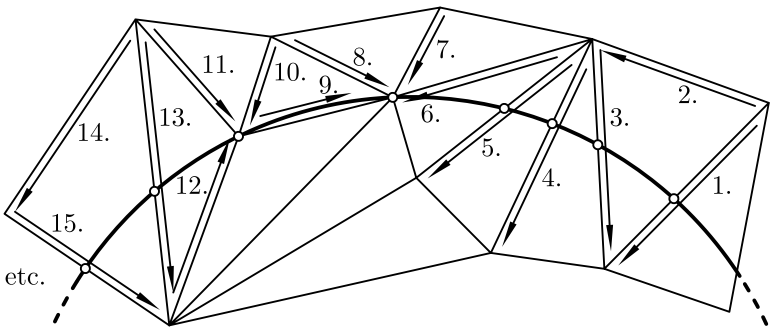

Figure 30: Algorithm (2.3) example

2.2.4 Step 4 — *golden section search*

If we want to find a zero of a function numerically there are several common methods, depending on the situation, for example Newton or Banach iteration. If we do not know the derivative of the function or there is none and we do not know a Lipschitz constant the most common method is binary search. It has only one demand to the function, that it is (strictly) monotonic.

As is generally known it works with an interval $[x_0, x_1]$, which contains the zero. If $\Psi(\frac{x_0+x_1}{2}) > 0$ (and Ψ is monotonically *increasing*) the zero must lie left of it and we change the interval to $[x_0, x_1] \mapsto [x_0, \frac{x_0+x_1}{2}]$, halfing its width. Analogously for the case $\Psi(\frac{x_0+x_1}{2}) < 0$.

The algorithm can terminate either if some evaluation produces a zero within some fixed tolerance, or if the interval width reaches a fixed lower limit.

Minima are of course zeros of the derivative of Ψ, but for Ψs that are not differentiable they can be found directly as well using a variation of binary search, *ternary search*.

The antiderivative of a monotonically increasing function is a convex function, so we might assume that these functions are those for which ternary search works. It turns out that a weaker assumption is sufficient:

We assume that Ψ is an *unimodal function*, that is a function $[a, b] \to \mathbb{R}$ that is (strictly) decreasing in $[a, m]$ and (strictly) increasing in $[m, b]$ for some $m \in [a, b]$. Obviously Ψ has a unique minimum at m. Figure (31) shows a function that is unimodal but not convex. It even need not be continuous.

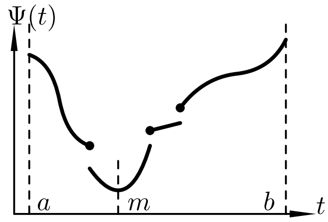

Figure 31: Unimodal function

From this follows that if for four points $x_0 < x_1 < x_2 < x_3$ we have $\Psi(x_1) < \Psi(x_2)$ the minimum cannot be $\in [x_2, x_3]$. Likewise, $\Psi(x_1) > \Psi(x_2)$ leads to $x_{\min} \notin [x_0, x_1]$.

So we can formulate an algorithm that in these cases cuts the right resp. left intervals and then evaluates Ψ at two further intermediate points of $[x_0, x_3]$ resp. $[x_1, x_4]$. We want to reduce this to a single additional evaluation per step by reusing one of the previous evaluations.

If we start, for example, with equally spaced points (x_0, x_1, x_2, x_3) we get, after a few iterations, intervals of very unequal lengths. This is detrimental to the speed of the algorithm. The ideal case would be that the ratios $(x_1 - x_0) : (x_2 - x_1) : (x_3 - x_2)$ stay constant for all iterations.

There is indeed a variant of ternary search that achieves just that. It is called *golden section search*. It was introduced by (J. Kiefer 1953) and realizes the best convergence rate possible for ternary search algorithms. The idea is that we let

$$(x_1 - x_0) : (x_2 - x_1) : (x_3 - x_2) = \varphi : 1 : \varphi \quad \text{where}$$
$$\varphi = \frac{1 + \sqrt{5}}{2} \text{ (the golden section)} \tag{89}$$

Algorithm 2.4. (Golden section search)

Input: Ψ unimodal, $[x_0, x_3]$ such that it contains a minimum of Ψ and a termination bound $\varepsilon > 0$.
$\varphi := \frac{1+\sqrt{5}}{2}$
$x_1 := x_0 + (2 - \varphi)(x_3 - x_0)$ and $x_2 := x_3 - (2 - \varphi)(x_3 - x_0)$
$f_1 := \Psi(x_1)$ and $f_2 := \Psi(x_2)$
loop
    if $f_1 < f_2$ **then**
        $x_3 := x_2$, then $x_2 := x_1$, then $x_1 := x_0 + x_3 - x_2$.
        $f_2 := f_1$, then $f_1 := \Psi(x_1)$.
    else
        $x_0 := x_1$, then $x_1 := x_2$, then $x_2 := x_3 + x_0 - x_1$.

    $f_1 := f_2$, then $f_2 := \Psi(x_2)$.
  end if
  if $x_3 - x_0 < \varepsilon$ **return** $\frac{x_1+x_2}{2}$ **end if**
end loop

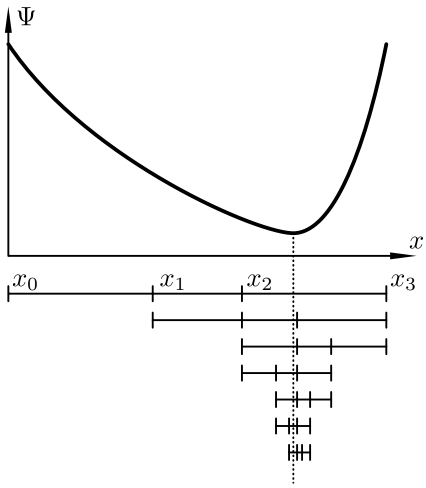

Figure 32: Example of *golden section search*

We see that in each step the interval length changes by

$$\frac{x_3' - x_0'}{x_3 - x_0} = \frac{\phi + 1}{\phi + 1 + \phi} = \phi^{-1} = \phi - 1 \approx 0.618, \tag{90}$$

for the prize of a single new evaluation of Ψ, which is quite good, considering that binary search has a factor of 0.5 per evaluation.

Considering this the termination condition could be rewritten to a fixed number of iterations.

There is a special case to be considered: If $\Psi(x_1) = \Psi(x_2)$, then the minimum must be $\in (x_1, x_2)$. In this case we could cut both the right and the left side intervals at the same time, that is

$$(x_0, x_1, x_2, x_3) \mapsto \big((x_1, x_1 + (2-\varphi)(x_2 - x_1), x_2 - (2-\varphi)(x_2 - x_1), x_2\big).$$

In this case the interval width changes by a factor of

$$\frac{x_3' - x_0'}{x_3 - x_0} = \frac{1}{2\varphi + 1} = 2\varphi - 3 = (\varphi - 1)^3$$

with, of course, two new evaluations of Ψ. As for the regular cases of cutting the left or the right side intervals the width changes by a factor of $\varphi - 1$, we see that the special case shortens the interval width as much as 3 regular steps for the prize of only 2 evaluations. We therefore spare one evaluation.

One the other hand, in particular because of the approximative nature of floating point algebra, the chances of this special case appearing in realistic situations are low. Therefore we will not implement it, to keep the algorithm simple as opposed to a slight time reduction in a very rare special case.

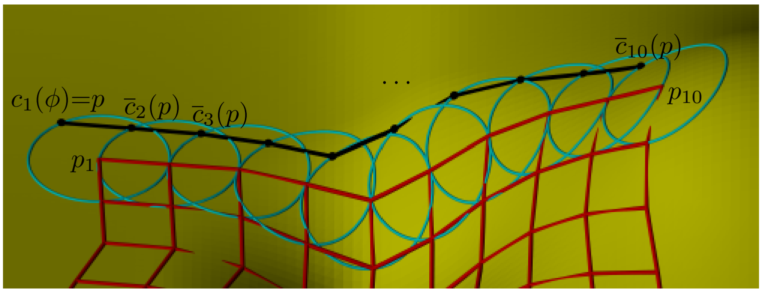

Figure 33: Task of step 4

Now we assume that we already have fixed a row $p_1, \dots, p_m \subset \mathcal{M}$ of knots of the rhombic net.

The algorithm in the previous section supplies the intersection curve of $\mathcal{M}$ and a sphere with radius r and its center $p_1 \in \mathcal{M}$. If the distance of p_1 and the edge of $\mathcal{M}$ is $> t$ then that curve is closed and, by theorem (2.3), goes "around" p_1, that is, if we assume the property of $\mathcal{M}$ that $z(f\rightarrow) \geq 2^{-1/2}\ \forall f \in \mathcal{F}_c$, then for every angle $\phi \in [0, 2\pi)$ there is a unique $r \geq 0$ and $\zeta \in \mathbb{R}$ such that $(r\cos\phi, r\sin\phi, \zeta)^T$ lies on the curve and the whole curve can be described that way.

Therefore the curve from section (2.2.3) has the form

$$c_1 \colon [0, 2\pi) \to \mathbb{R}^3,\ \phi \mapsto p_1 + \begin{pmatrix} r(\phi)\cos\phi \\ r(\phi)\sin\phi \\ \zeta(\phi) \end{pmatrix}, \tag{91}$$

where $r(\phi) \in [r/\sqrt{2}, r]$ and $\zeta(\phi) \in [-r/\sqrt{2}, r/\sqrt{2}]$ are both 2π periodic continuous functions.

Of course the first rhombic knot of the new row of knots will $c_1(\phi)$ for some ϕ. We fix a unique ϕ_0 such that $c_1(\phi_0)$ is the optimal position for the new rhombic net knot. Such a condition might be for example

$$p_{11} - p_1 \perp p_2 - p_1, \text{ if the first new knot is called } p_{11}.$$

Then we fix an evaluation function $\Psi_1\big(c_1(\phi)\big) := \big|\psi_1(\phi - \phi_0)\big|$ for some strictly monotonic continuous function ψ_1 with $\psi_1(0) = 0$. This makes Ψ_1 a unimodal function.

Likewise we use the algorithm in the previous section to calculate the curves around $p_2, \dots, p_m$ and fix optimum positions for new knots and evaluation functions $\Psi_2, \dots, \Psi_m$.

There are various possible choices for Ψ_i, they may even be different for different i, but the most simple choice is

$$\Psi_i\big(c_i(\phi)\big) = \big|\arctan(\phi - \phi_i)\big|, \tag{92}$$

which can be evaluated without further use of trigonometric functions after some preliminary calculations, because by algorithm (2.3) $p = c_i(\phi)$ is not given in terms of an angle ϕ, but as a vector $\in \mathbb{R}^3$.

$$\Psi_i(p) = \left|\frac{\langle p - p_i, \varepsilon_1\rangle}{\langle p - p_i, \varepsilon_2\rangle}\right|, \text{ where } \varepsilon_1 = \operatorname{rot}_{\phi_i}^{e_3} e_2 \text{ and } \varepsilon_2 = \operatorname{rot}_{\phi_i}^{e_3} e_1. \tag{93}$$

Of course these evaluation functions are only defined for $|\phi - \phi_i| < \pi/2$, but in practical situations we only need them in that interval, so it is not a problem.

Lemma 4. *Let f_1 and f_2 be two continuous unimodal functions $[a, b] \to \mathbb{R}$. Then $x \mapsto \max\{f_1(x), f_2(x)\}$ is also a continuous unimodal function.*

Proof. Let m_1 and m_2 be the unique minima of f_1 and f_2. Assume w.l.o.g. $m_1 \leq m_2$. Then $f(x) := \max\{f_1(x), f_2(x)\}$ is monotonically decreasing in $[a, m_1]$, as $x < x' \Rightarrow f_1(x) > f_1(x') \wedge f_2(x) > f_2(x') \Rightarrow f(x) > f(x')$, and likewise monotonically increasing in $[m_2, b]$.

In $[m_1, m_2]$ f_1 is increasing and f_2 is decreasing. If $f_1 - f_2$ is positive in the whole interval, then the unique minimum of f is at $m := m_1$ and $f = f_1$ in $[m_1, m_2]$, therefore monotonically increasing. The situation is analogous in the case $f_1 - f_2 < 0$ on $[m_1, m_2]$.

If $[m_1, m_2]$ contains positive and negative values of $f_1 - f_2$, then the intermediate value theorem gives us a point $m \in [m_1, m_2]$ with $f_1(m) = f_2(m) = f(m)$. The fact that f_1 is increasing and f_2 is decreasing in the interval shows that f increases right of m and decreases left of it. □

The assumption of the functions being continuous is necessary as the following example demonstrates:

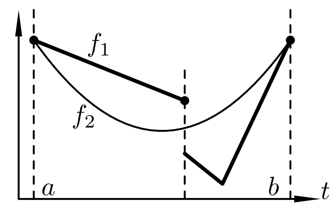

Figure 34: Maximum of discontinuous unimodal functions

The maximum of those two functions does not have a minimum, only an infimum which is not a function value, and therefore the function cannot be unimodal. This is the reason for having demanded that the evaluation functions Ψ_i are continuous, as we now define

$$\Psi(p) := \Psi\big(p, \bar{c}_2(p), \ldots, \bar{c}_m(p)\big) := \max\big\{\Psi_1(p), \Psi_2(\bar{c}_2(p)), \ldots, \Psi_m(\bar{c}_m(p))\big\}. \tag{94}$$

There is a fundamental problem here. The functions $\bar{c}_2, \ldots, \bar{c}_m$ continuously map the curve around p_1 onto those around $p_2, \ldots, p_m$ under the condition

$$\|\bar{c}_2(p) - p\| = r \text{ and } \|\bar{c}_i(p) - \bar{c}_{i-1}(p)\| = r \text{ for } i = 3, \ldots, m \tag{95}$$

The problem is that there is no way to make sure the $\bar{c}_i$ are injective. They generally never are if defined on the whole curve around p. We will be only needing them on a certain section of the curve that we expect to contain the desired optimum point. This takes care of the main violations of injectivity, but there can still be constructed examples of surfaces with non-injective $\bar{c}_i$ even for arbitrarily flat surfaces (so the condition on $\mathcal{M}$ from the previous section will not help), in which case $\Psi_i \circ \bar{c}_i \circ c_1$ will not be unimodal. But it turns out that in reasonable practical situations (in particular, if r is not too large) they are injective in the desired range, so the algorithm will work.

The evaluation of $\overline{c}_i$ will not be shown in detail here, but it boils down to the solution of quadratic equations.

We can now fix an arbitrary continuous bijective parametrization of the curve $p = c_1(\phi)$ (by c_1 or any other function f) and put $\Psi \circ f$ into the golden section search algorithm to find the unique minimum.

3 Possible applications

3.1 Rhombic-conical nets

The main practical application for rhombic nets is without doubt architecture.

The degrees of freedom of a rhombic-conical net in chosing the angle mappings ϕ and θ, the start angle σ_{11}, the cone aperture Ω and the wrenching angle α allow the construction of æstetically pleasing nets, though of course with severe constraints as opposed, e.g., to NURBS surfaces.

For example, (Schneider-Schätzke-Hegger-Voss 2006) demonstrated a way of constructing rhombic net lattices out of pre-fabricated concrete segments each constituting a single rhombus face. In this solution all the rhombi are identical which for reasons of symmetry makes the resulting surface a rhombic net with conic knots of uniform aperture and, in particular, a cylindrical surface. The downside of this method is obviously that it is limited to cylindrical, planar and spherical surfaces.

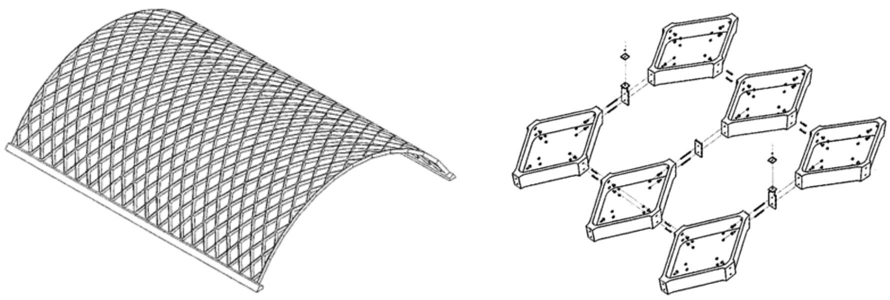

(a) Complete cylindrical lattice

(b) Assembly of segments

Figure 35: Pre-fabricated concrete lattice (images from (Schneider-Schätzke-Hegger-Voss 2006))

We will now show more general ways of constructing rhombic nets.

The nice thing about rhombic-conical nets is that if we consider triples of edges together with the two adjacent cone normals there are only two different kinds, even if ϕ and θ are not constant. This would mean we need only two edge parts.

The edge components are fixed onto bolts that constitute the knot normals. The holed ears of the edges that slide onto the bolts need to be stacked onto each other. This makes it neccessary to shift the ears up- and downwards along the knot axis relative to the edges to make room for them. There is an arrangments for this that needs only four different kinds of edges. Even more: If it is possible to use edge components in a flipped position as well (if, e.g. there are no appendages for the attachment of plates on only one side or similar), this number can be reduced to only two. Figure (36) illustrates this, as the fourth and first as well as the second and third bars are identical.

Figure (37) shows how a small part of such a lattice may look like when assembled.

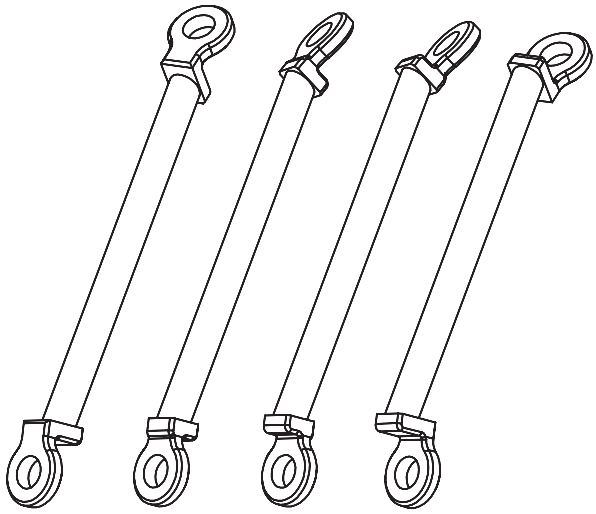

Figure 36: 4 types of bars

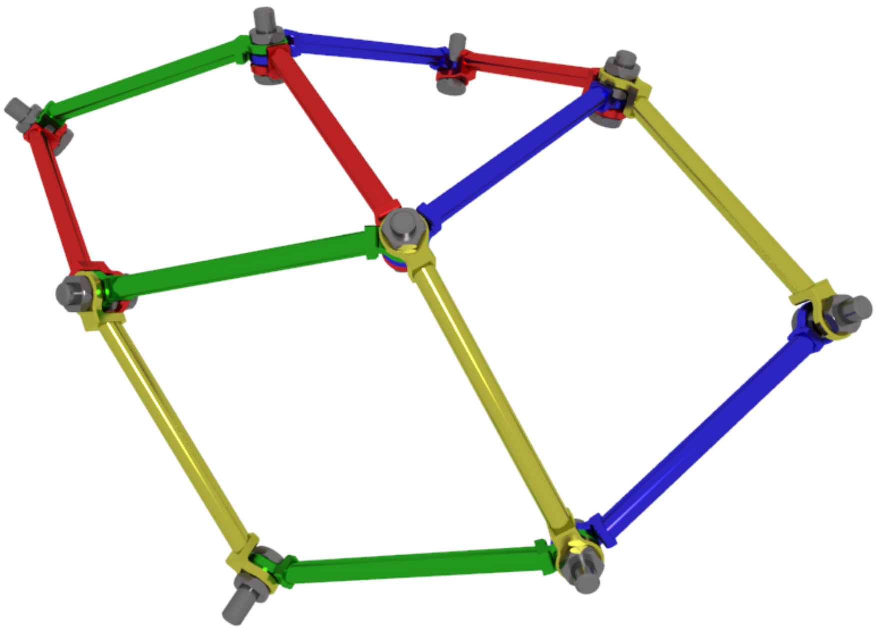

Figure 37: Realization of a rhombic-conical net

3.2 General rhombic nets

General rhombic nets that are constructed as approximations of smooth surfaces promise to be more fruitful for use by architects, as the normal approach of constructing surfaces without mathematical constraints and only converting them into rhombic nets afterwards can be retained.

As general rhombic nets do not have conic knots, let alone such with uniform aperture, from which follows that the rhombi do not have uniform wrenching angles either. This means that we have two options in physically building such nets. We can either taylor-make each rhombic edge (which can be several thousands) or build each edge from several linked parts that allow different angles. We will now show several variations of realizing the second approach.

The central problem is that rhombic edges must be able to freely swivel around rhombic knots. Usually things like that can be realized by ball joints, but in our situation four edges meet in each knot which together with the fact that the angles between edges vary in a wide range forbids the use of ball joints. Therefore we will be using variants of Cardan joints. Once all the edges are positioned the links can be immobilized by screws or welds.

The first step is to fix a normal in each rhombic knot. This can be done in several different ways which are discussed in detail later. This normal serves as the axis of a bolt, onto which coupling parts are placed. As in the previous section there are four different ones or, if symmetries are exploited, two different ones, to keep the horizontal Cardan axes of the four edges at a uniform height (in a common plane). Figure (38) and figure (39) show two possible technical solutions. The four different coupling parts are shown in different colors, where green and cyan, as well as red and yellow are identical, just flipped. The central bolts are not shown in the drawings.

The difference between the two variants is in the way the horizontal axes are realized. The first one (figure (38)) moves the joint along the axis away from the center (where the four horizontal axes intersect).

The second one replaces the horizontal axes with a bent prismatic joint such that the piston part in sliding swivels around the theoretical axis (figure (39)).

To make it possible for edges to have different wrenching angles each edge is split in two half edges which are joined in the middle of the edge by a coaxial bolt. All in all these solutions need two kinds of bolts, one kind of half edge and four, resp. two coupling parts.

Figure (40) and figure (41) show the same rhombic net realized by each variant.

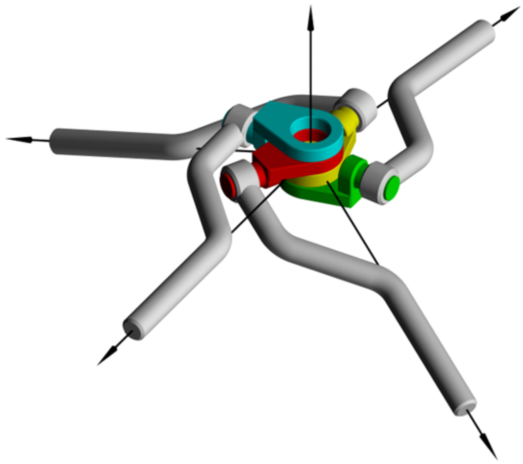

Figure 38: General rhombic net — variant 1

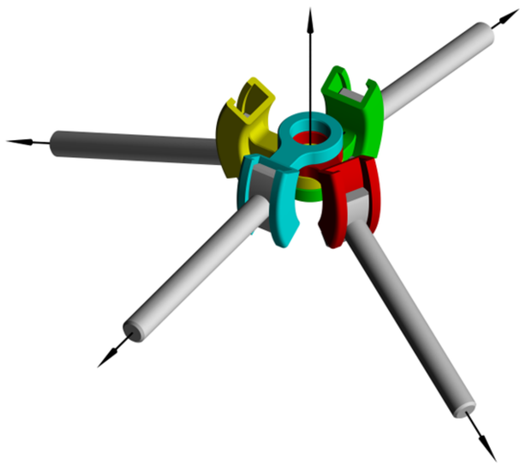

Figure 39: General rhombic net — variant 2

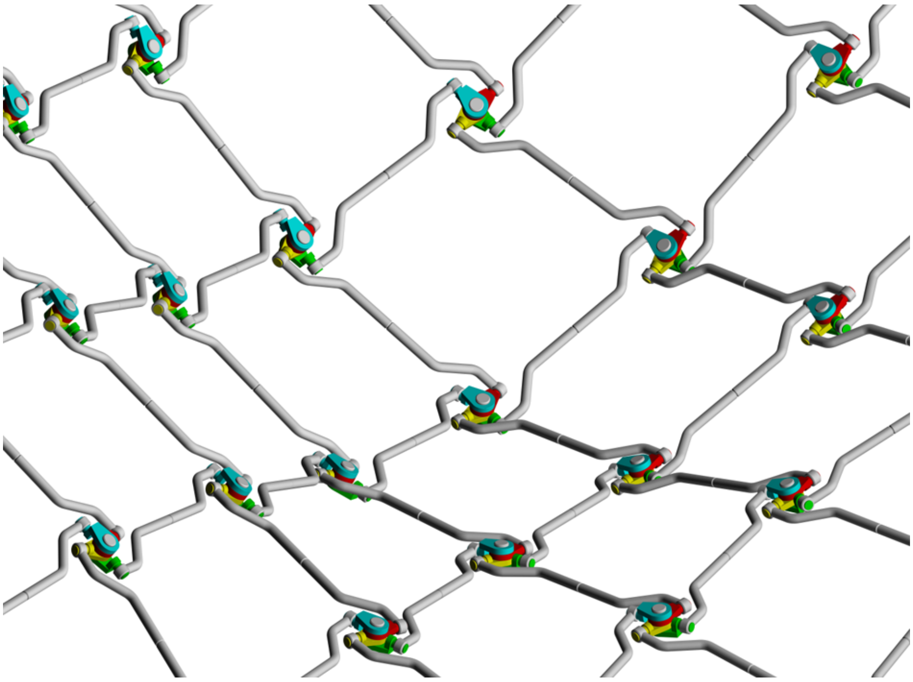

Figure 40: General rhombic net — variant 1

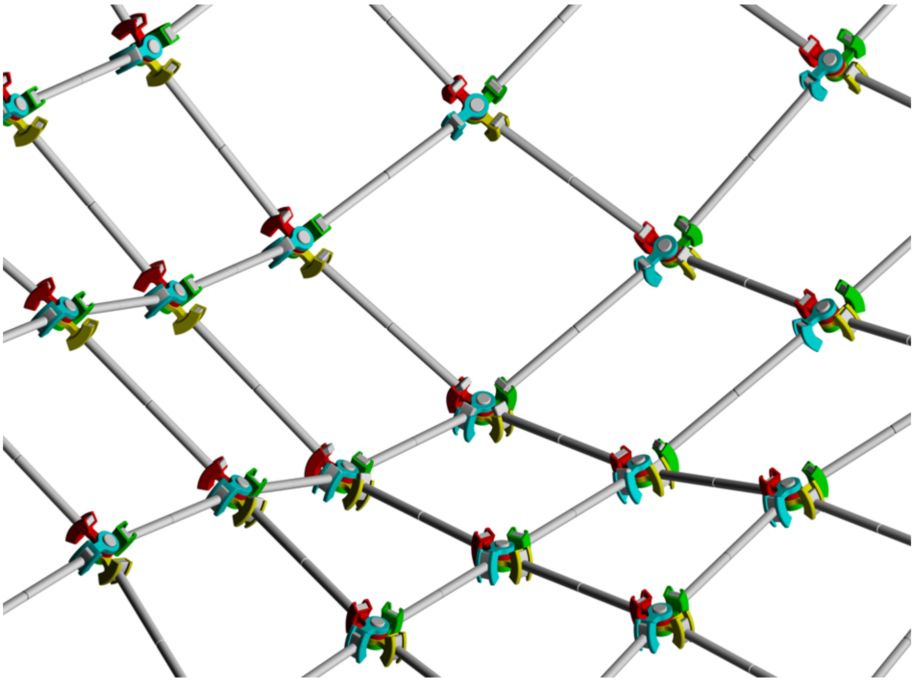

Figure 41: General rhombic net — variant 2

3.3 Approximated rhombic nets

Obviously the realization possibilities suggested in the previous section are rather complicated. In particular they might be problematic from the point of view of statics. This sections shows a possible way to deal with this issues.

The idea is to abandon the requirement that the axes of the bars that represent the rhombic edges exactly coincide with the theoretical rhombic edges. This has the advantage that the four bars in each knots need not intersect and therefore there is room enough for simple joints, in particular ball joints.

The downside is that the bars generally will not have uniform length any more. But it turns out that the differences are small enough ($< 1\%$ in the example below) to be compensated by slide joints or adjustment screws in the middle of the bars.

The whole assembly of a bolt and four coupling parts is replaced by a single part with four ball joint sockets spaced radially by 90° each (and with its symmetry axis being the knot normal, of course). See figure (42b).

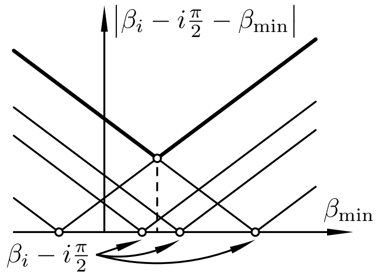

(a) Proof of lemma (5)

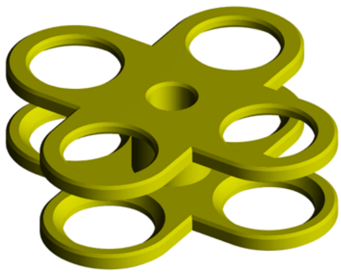

(b) Ball joint socket

Figure 42: circular quadrilaterals

There are two kinds of deviation from the theoretical net here. One is of course that the bar axes which go through the center of the respective joint balls do not intersect in the center of the socket component. The other one is that the ball centers do not lie on the planes spanned by n and $\delta_i f$, as the ball centers are spaced by 90° and the $\delta_i f$ are generally not. But we will rotate the socket component around n by such angle $\beta_{\min}$ that the deviations are minimal. For this we project the $\delta_i f$ onto the knot plane and calculate their angles $\beta_i \in [0, 2\pi)$ with $\delta_2 f$ having the angle 0.

Lemma 5. *Let the angles $\beta \in [0, 2\pi)$, $i = 1, 2, 3, 4$. Then the angle β_{min}, defined as the angle such that $\max_{i\in\{1,\dots,4\}} \left|\beta_i - (i\frac{\pi}{2} + \beta_{min})\right|$ attains a minimum, is given by*

$$\beta_{min} = \frac{1}{2}\Big(\min_{i\in\{1,\dots,4\}} \big(\beta_i - i\frac{\pi}{2}\big) + \max_{i\in\{1,\dots,4\}} \big(\beta_i - i\frac{\pi}{2}\big)\Big). \tag{96}$$

Proof. $\left|\beta_i - i\frac{\pi}{2} - \beta_{\min}\right| = \max\left\{\beta_i - i\frac{\pi}{2} - \beta_{\min}, -\beta_i + i\frac{\pi}{2} + \beta_{\min}\right\}$ and therefore

$$\begin{aligned}\max_i \left|\beta_i - i\frac{\pi}{2} - \beta_{\min}\right| &= \max\Big\{\max_i \big(\beta_i - i\frac{\pi}{2} - \beta_{\min}\big), \max_i \big(-\beta_i + i\frac{\pi}{2} + \beta_{\min}\big)\Big\} = \\ &= \max\Big\{-\beta_{\min} + \max_i \big(\beta_i - i\frac{\pi}{2}\big), \beta_{\min} - \min_i \big(\beta_i - i\frac{\pi}{2}\big)\Big\}\end{aligned}$$

As one of the two terms falls with $\beta_{\min}$ and the other one increases the maximum is minimal when both terms are equal and therefore

$$\max_i \left(\beta_i - i\frac{\pi}{2}\right) + \min_i \left(\beta_i - i\frac{\pi}{2}\right) = 2\beta_{\min}. \qquad \square$$

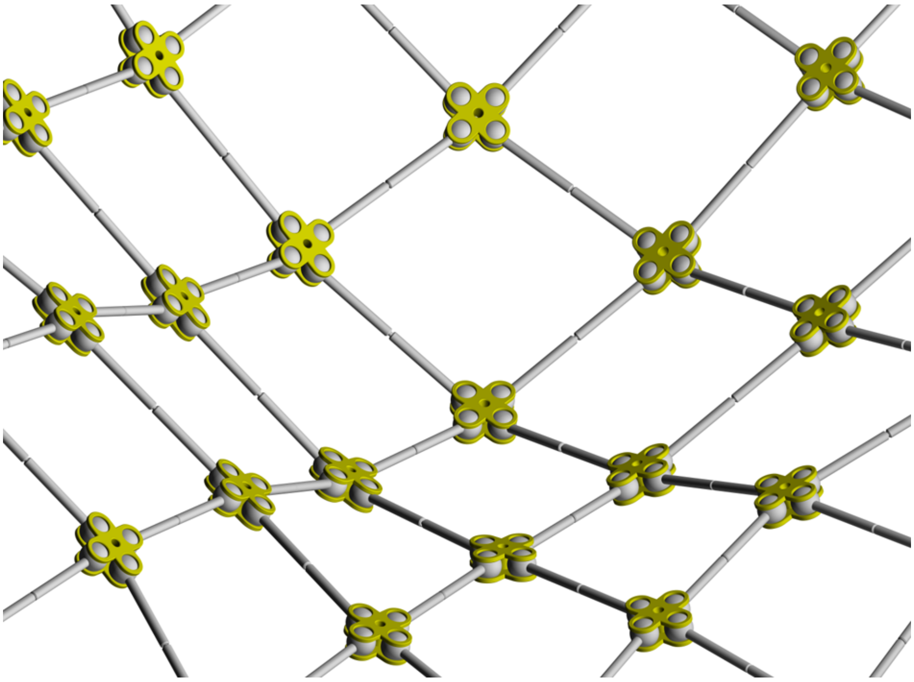

Figure 43: General rhombic net — approximated

References

Bobenko, A.I. and Y.B. Suris, *Discrete Differential Geometry: Integrable Structure*, American Math. Soc., 2008

Kiefer, J., Sequential minimax search for a maximum, Proc. Am. Math. Soc. **4** (1953), no. 3, 502–506

Liu, Z., H. Pottmann, J. Wallner, Y.-L. Yang and W. Wang, *Geometric modeling with conical meshes and developable surfaces*, ACM Trans. Graphics **25** (2006), no. 3, 681–689, Proc. SIGGRAPH

Wunderlich, W., *Zur Differenzengeometrie der Flächen konstanter negativer Krümmung*, Sitzungsber. Österr. Akad. Wiss. **160** (1952), 39–77

Weiler, K., *Edge-based data structures for solid modeling in a curved surface environment*, IEEE Comput. Graph. Appl. **5(1)** (1985), 21–40.

Mäntylä, M., *An Introduction to Solid Modeling*, Computer Science Press, Rockville, MD, 1988

Schneider, H.N., C. Schätzke, J. Hegger and S. Voss, *Structure construction/rhombic lattice structures. Bar nets of textile reinforced concrete*, BFT International **72** (2006), no. 3, 34–40